REAL TIME NMR ANALYSES OF PHENOLIC RESIN REACTIONS

A thesis submitted in partial fulfilment

of the requirements for the degree

of

Master of Science in Chemistry

at

The University of Waikato

by

SAMUEL LINDSAY WOOLLEY

The University of Waikato

Te Whare Wānanga o Waikato

February 2008

Abstract

The current investigation presents the development and application of a “Rapid” NMR acquisition method, capable of identifying transient species and quantitatively monitoring their changes in real time during an *in situ* phenolic resin preparation. This quantification was only possible after the determination of phenolic resin relaxation times (T_1) and nuclear Overhauser enhancements (NOE).

Rapid NMR spectra were recorded with an inter-pulse delay time of 0.6 s and broadband decoupling, which resulted in the acquisition of sequential qualitative spectra at 2.5 min intervals. The obtained qualitative spectral data were then converted into quantitative spectral data via the derived cross calibration (f_c) and NOE (η) factors, resulting in quantitative reaction profiles for the phenoic resin species under investigation.

Extension of this work will allow the effects of varying synthesis parameters (i.e. temperature, pH, stoichiometry, catalyst type, etc.) on the final structure and hence on the final physical properties of the resin to be determined and inevitably leading to the development of new, more innovative and cost-effective resins.

Acknowledgements

I would like to express my appreciation to my Waikato supervisors, Dr Michael Mucalo, Associate Professor Alan Langdon and Professor Alistair Wilkins, for their encouragement and advice throughout the project.

I would wish to thank my industry based supervisor Clyde Campbell, for stimulating discussions and guidance throughout the project, and also Scott Earnshaw and Alex Bruce for technical suggestions throughout the project.

A further mention of thanks is required for the University of Waikato's Chemistry department and especially, Pat Gread, Jannine Sims and Annie Barker for providing the necessary chemicals, lab equipment and instrumental training.

Financial assistance was provided by the Foundation for Research Science and Technology through a technology in industry fellowship (TIF) in collaboration with Hexion Specialty Chemicals and is greatly acknowledged.

Finally, I wish to thank my family for their ever enduring encouragement and support.

Table of Contents

List of Tables

List of Figures

List of Abbreviations

ATR	Attenuated total reflectance spectroscopy
AQ	Acquisition time
C:P	Caustic to phenol ratio
DEPT	Distortionless enhancement by polarisation transfer
DMP	Dimethylol phenol
DPHF	Diphenolic hemiformal
ES-MS	Electrospray ionisation mass spectroscopy
FT-IR	Fourier transform Infrared spectrometry
F:P	Formaldehyde to phenol ratio
GPC	Gel permeation chromatography
HPLC	High performance liquid chromatography
MALDI-TOF	Matrix assisted laser desorption ionisation time-of-flight
MP	Methylol phenol
NMR	Nuclear magnetic resonance
NS	Number of scans
NOE	Nuclear Overhauser enhancement
PHF	Phenolic hemiformal,
PW	Pulse width
TMP	Trimethylol phenol
VTU	Variable temperature unit

List of Symbols

B_0	Static magnetic field
M_0	Equilibrium magnetisation
μ	Magnetic moment
γ	Gyromagnetic ratio
v_0	Frequency of precession
f_C	Cross calibration factor
η	NOE factor
D_1	Repetition delay (sec)
T_1	Longitudinal relaxation time (sec)
I	Intensity of the observed NMR signal
θ	Excitation pulse angle
S/N	Signal to noise ratio
Φ	A phenolic moiety
M_z	The sample magnetization
τ	Delay time
I_τ	Intensity after delay time τ
I_∞	Intensity after delay time ∞
f_{NS}	Number of scans correction factor

1 Introduction

1.1 GENERAL INTRODUCTION

More than a century has passed since the discovery and commercial exploitation of phenol formaldehyde (phenolic) resins[1]. The techniques originally proposed by Baekeland[2] made possible the worldwide application of the first wholly synthetic polymer material.

Since then, the global thermoset resins market has become a large enterprise with recent (2007) annual sales reaching approximately $34 billion ($US).[3] However this value is not restricted to phenolic based resins and includes other thermosetting resins such as amino and epoxy resins. Approximately 16000 tonnes of phenolic resin are sold on the New Zealand market per annum.

Since their development, a large body of scientific literature has become available with a number of text books devoted entirely to phenolic resins.[1, 4, 5] Brief accounts of the chemical reactions involved, commercial importance, and application of phenolic resins can be found in almost any text book involving synthetic resins, plastics or polymers.[6-9]

Phenolic resins play a significant role within the polymer industry providing a diverse range of products with an equally diverse range of applications. Phenolic resins are commonly used as moulding compounds in foundry, spray insulators, and lacquers and varnishes. The phenolic resins relevant to this investigation are those as used in the wood adhesives industry for the production of plywood and laminated veneer lumber (LVL).

Phenolic resins provide substantial advantages over other formaldehyde based resins (e.g. urea formaldehyde resins) such as superior strength and resistance to hydrolysis (water). These properties are due to the rigid carbon-carbon network within the resin structure. Hydrolysis of formaldehyde based resins leads to the release of formaldehyde, a major problem associated with urea based formaldehyde resins. Hence phenolic resins find applications in more demanding environments such as outdoor building materials and in construction.

The major limitation of phenolic resins is the cost associated with manufacture. The raw materials are not only more expensive to source, but they require more energy demanding conditions, than those of urea formaldehyde resins, to produce.

Continued improvements are required to produce and hence supply commercial resins that are more efficient and more economical, while maintaining (or enhancing) the final physical properties which make phenolic resins such a popular choice.

Further development has therefore necessitated a more complete understanding of how these resins function. A significant amount of research into the chemistry of the resin synthesis is required to achieve such an understanding.

In previous research the structure resolving properties of NMR allowed Zeng[10] to develop an in situ NMR acquisition method capable of investigating the reactions between urea and formaldehyde in real time. Further development and application of this method to the complex phenol formaldehyde reaction, in order to obtain a greater understanding of the polymerisation processes taking place, will serve as the primary focus of this thesis.

The work thus requires an understanding of the chemistry of phenol formaldehyde resins and Nuclear Magnetic Resonance spectroscopy (NMR). An introduction of these topics will be covered in the next sections.

1.2 THE CHEMISTRY OF PHENOL FORMALDEHYDE RESINS

1.2.1 Raw Materials

Phenol

Phenol occurs naturally in coal tar, however, natural phenol accounts for only a small proportion of the total world production, with the majority being synthesised from benzene[1]. The process of which is known as the "Cumene" or "Hock" process and an overview of the reaction follows (Equation 1.1):

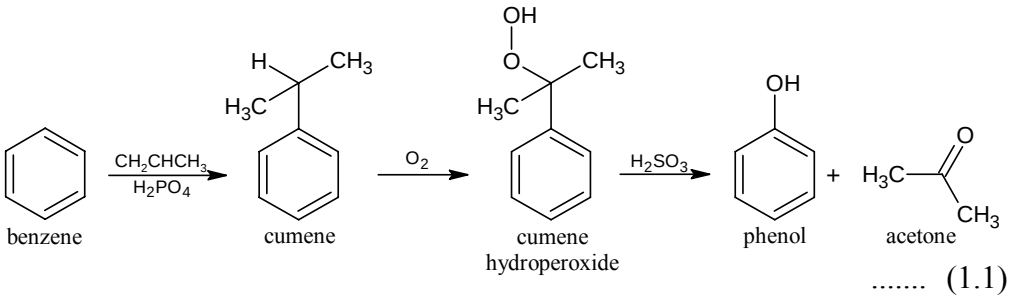

..... (1.1)

The cumene (isopropylbenzene) required for the process is produced by alkylation of benzene with propylene using a solid phosphoric acid catalyst. Cumene in the liquid phase is oxidised in air to form cumene hydroperoxide. Concentration of cumene hydroperoxide and separation of the unreacted cumene occur during the second stage of the process. The concentrated reaction product is then converted in a splitting plant using sulphuric acid as a catalyst to a crude mixture of phenol and acetone, which is treated with various purification and distillation steps.

At least 95% of the commercial phenolic resins are based on phenol itself. For the remainder, other phenols i.e. cresols, xylenols and resorcinols, are utilised in order to confer specific properties, such as alkali-resistant resin grades and cold-setting adhesives.

Formaldehyde

Formaldehyde is commonly produced from methanol over a silver catalyst[1]. The methanol is partially oxidised and dehydrogenated on silver crystals as a vapour/methanol/air mixture. The conversion from methanol to formaldehyde (Equation 1.2) is considerably high at approximately 90%.

$$CH_3OH + ½\ O_2 \longrightarrow CH_2O + H_2O \quad \text{..... (1.2)}$$

The reaction mixture and air is prepared so as to be over the upper flammability limit. Reactor effluent passes to the absorption train, where formaldehyde and other consumables are recovered by condensation and absorption in re-circulating formaldehyde streams. The raw formaldehyde is then purified by stripping the unconverted methanol.

In aqueous medium a very fast acid and base catalysed hydration reaction of formaldehyde to methylene glycol occurs (Equation 1.3).

$$nCH_2{=}O + H_2O \rightleftharpoons HOCH_2OH \quad \text{..... (1.3)}$$

$$nHOCH_2OH \rightleftharpoons HO(CH_2O)_nH + nH_2O \quad \text{..... (1.4)}$$

The equilibrium lies almost exclusively to the right (Equation 1.3) and hence aqueous formaldehyde exists almost exclusively as methylene glycol and its polymeric forms (as shown in Table 1.1 and Equation 1.4). The concentration of monomeric formaldehyde is typically very low < 0.01%.

Table 1.1: A table showing the molecular weight distribution of the polymeric methylene glycol species ($HO(CH_2O)_nH$) present within an aqueous solution of formaldehyde (40% at 35ºC)[1].

n	%	n	%
1	26.81	6	5.88
2	19.36	7	3.87
3	16.38	8	2.50
4	12.32	9	1.58
5	8.96	10	0.99

The depolymerisation of aqueous polymeric methylene glycols (Equation 1.5), in the presence of acid and base type catalysts becomes important for the overall reaction rates for phenolic resin formation:

$$HO(CH_2O)_nH + H_2O \rightleftharpoons HO(CH_2O)_{n-1}H + HOCH_2OH \quad \text{.....} \quad (1.5)$$

Further (minor) stabilisation equilibria exist in the presence of methanol, where methylene glycol type species react to form hemiacetals and their associated polymeric derivatives (Equation 1.6). The below equilibrium lies well to the right in acidic environment, however in a basic environment the position of the equilibrium is reversed leading to the production of methanol:

$$CH_3OH + HO(CH_2O)_nH \rightleftharpoons CH_3OCH_2O(CH_2O)_{n-1}H + H_2O \quad \text{....} \quad (1.6)$$

By the catalytic action of strong bases formaldehyde undergoes a disproportionation reaction known as the Cannizzaro reaction (Equation 1.7); and hence small amounts of formate are usually present.

$$2CH_2{=}O + NaOH \rightleftharpoons CH_3OH + H(CO)O^-Na^+ \quad \text{.....} \quad (1.7)$$

1.2.2 The Reaction between Phenol and Formaldehyde

In industry phenolic resin reactions are usually carried out in two separate operations. The first operation involves the formation of a low molecular weight, fusible, soluble pre-polymer resin. These reactions are carried out batch wise on a scale of about 16 tonnes. The second operation involves curing reactions which lead to the final infusible cross-linked product.

Two distinct classes of phenolic resins exist; namely Novolac's and Resole's. The major differences between these two classes are the formaldehyde to phenol (F:P) ratio and the type of catalyst used.

Novolac resins

Novolac phenolic resins are prepared by the interaction of a molar excess of phenol with formaldehyde under acidic conditions. Novolacs are thermoplastic and are characterised structurally by the absence of methylol type groups. These resins are generally insoluble in water, soluble in low molecular weight alcohols and have an indefinite shelf life. In order to convert novolacs into network polymers (i.e. cure) an addition source of formaldehyde (as a cross linking agent) is required i.e. hexamethylenetetramine.[6]

A second class of Novolac resins exist which is prepared between the pH range of 4 to 7 and employ catalysts such as zinc acetate. These are referred to as high *ortho*-novolacs and cure rapidly when heated in the presence of a formaldehyde source.

Resole resins

Resole phenolic resins are usually prepared by the interaction of a molar excess of formaldehyde with phenol under alkaline conditions. They are cured by heat and belong to the thermosetting class of polymers. Three individual stages of the reaction need to be considered when dealing with resole type phenolic resins. They are: addition, condensation and cure.

Resole type phenolic resins are of major importance of the present investigation, as these resins are commonly employed in the plywood and LVL industries for which this research is ultimately directed.

The chemistry involved in the formation of resole type phenolic resins has largely been dealt with in the literature[1, 4-6]. There are three stages to the synthesis:

1. Additon Stage Reactions

The addition stage reactions are generally considered to be those forming the simple mehylol phenols. In the presence of alkali phenol reacts to form the resonance stabilised phenoxide anion (Equation 1.8):

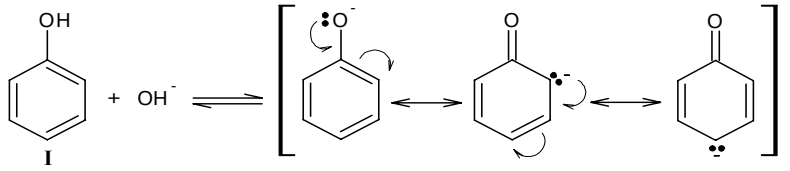

I ..... (1.8)

This activated phenoxide ion is more reactive and more *ortho*-/*para*- directing in alkaline solution than phenol in neutral or acidic solution. Thus activated phenol reacts directly with aqueous formaldehyde to form the *ortho* and *para* methylol phenols (Equations 1.9 and 1.10 respectively):

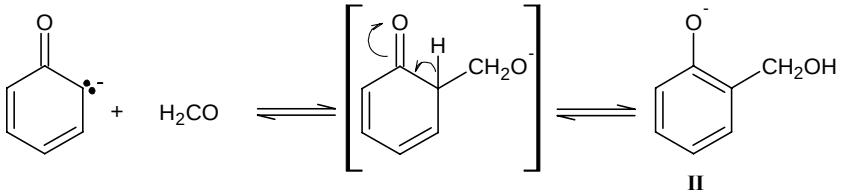

II ..... (1.9)

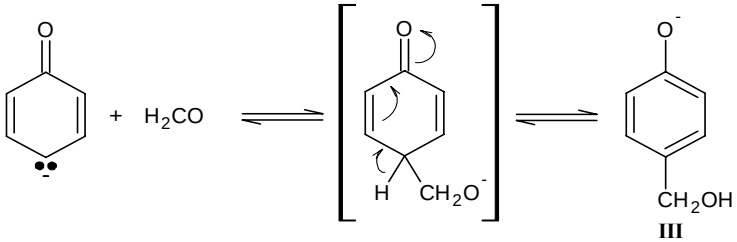

III ..... (1.10)

The above reactions have been somewhat simplified as the actual hydroxylalkylating species has not been mechanistically established in the literature[6]. Hence it is not completely understood how formaldehyde, as methylene glycol (see Section 3.2.1) reacts with the phenoxide ion. For sake of clarity the simple formaldehyde molecule has been shown.

The resulting *ortho* and *para* methylol phenols are more reactive towards formaldehyde than the original phenol and rapidly undergo further substitution to form the di- and tri-methylol derivatives (Equations 1.11 – 1.13):

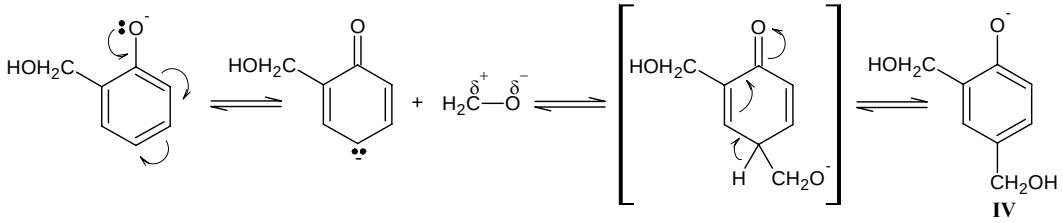

..... (1.11)

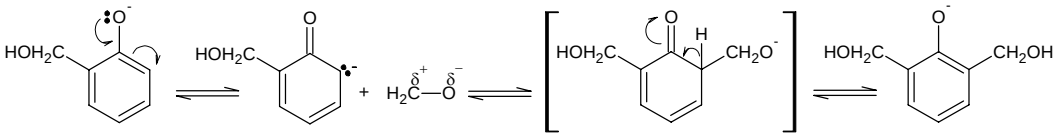

..... (1.12)

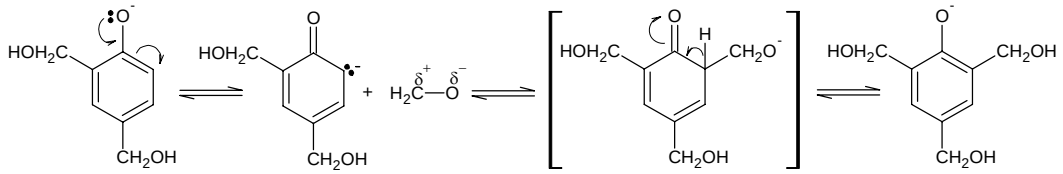

..... (1.13)

Once the substituted phenolic monomers become involved the disappearance of phenol is delayed. Hence the methylol phenols and the un-reacted phenol compete to react with the available formaldehyde.

A generalised scheme of all the overall possible reactions leading to the simple methylol phenols, including relative rates of formation[11] is presented below (Equation 1.14):

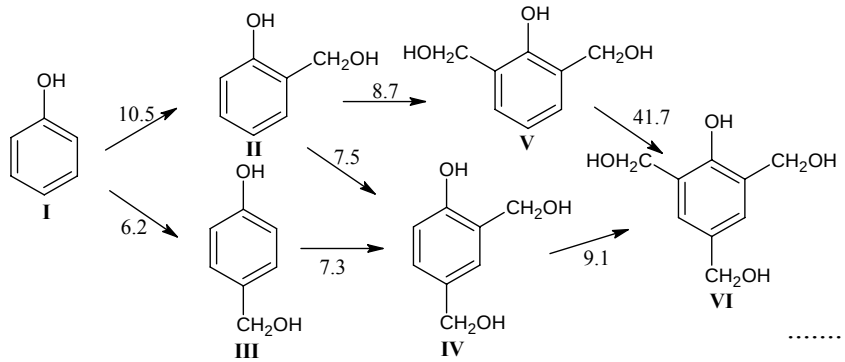

..... (1.14)

2. Condensation Stage Reactions

The methylol phenols obtained are relatively stable in the presence of alkali but can undergo self-condensation to form dinuclear and polynuclear phenols in which the phenolic nuclei are linked by methylene groups.

These self condensation products can arise from the two available mechanisms. The first involves the attack on a methylol group by an unsubstituted *ortho* or *para* position of the phenolic ring with the displacement of a hydroxyl group (Equation 1.15 and 1.16). The second involves the interaction of two methylol groups with the displacement of a hydroxyl group, followed by the subsequent elimination of one of these methylol groups as formaldehyde (Equation 1.17).

The reactions below are shown for the mono substituted methylol phenols for sake of clarity. Similar reactions occur for the di- and tri- methylol phenols.

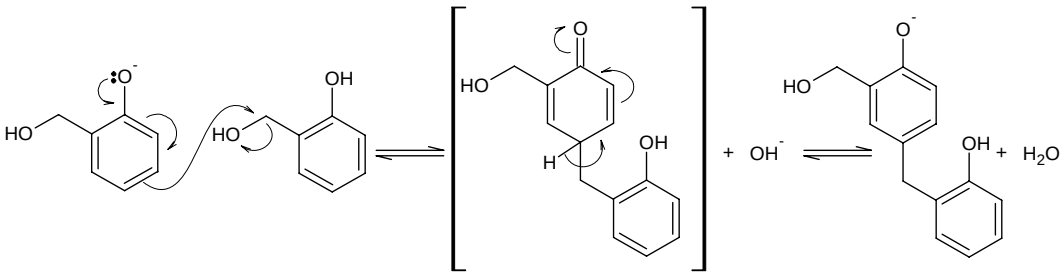

..... (1.15)

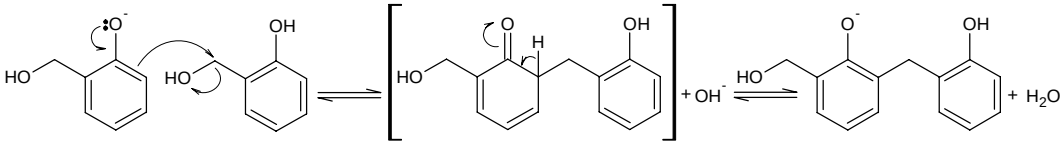

..... (1.16)

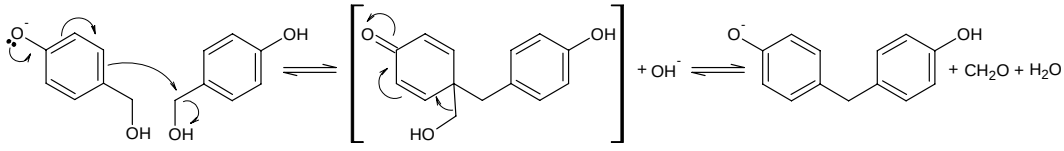

..... (1.17)

Under the condensation stage conditions, employed in the present investigationl the mechanisms available do not promote the formation of *ortho,ortho*-methylene linkages (Equation 1.16) but are included here for completeness.

The diphenyl methanes (Equations 1.15 and 1.17) can further react to form tri-nuclear and higher order poly-nuclear phenols, linked with *ortho,para*- or *para,para*-methylene bridges (Equation 1.18).

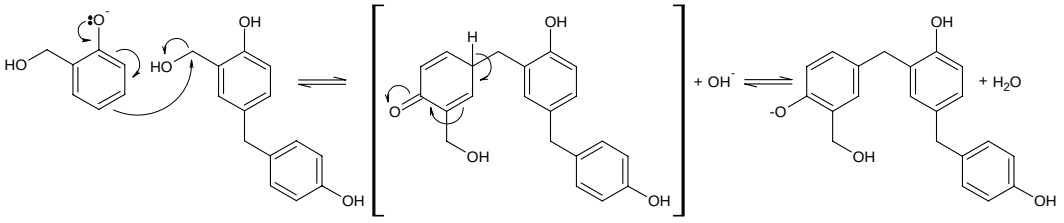

..... (1.18)

The above reactions lead to a proposed structure of the final liquid resole phenolic resin (Figure 1.1) which describes a mono or polynuclear phenol, with three possible substituents. These substituents will be some combination of methylol type species and phenolic rings bound by *ortho,para*- or *para,para*- methylene bridges.

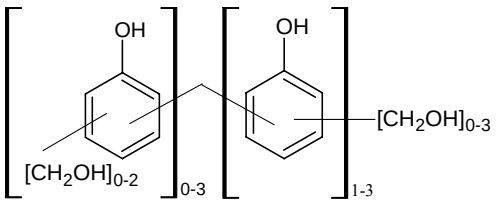

Figure 1.1: A proposed structure of a final liquid state resole resin.

3. Curing Reactions

The reactions by which resoles are transformed further into high molecular weight, cross linked (i.e. cured) materials are extremely complex and involve a number of competing reactions.

The transformation may be accomplished by simply heating a resin and it is generally unnecessary to add any further reagent. The preparation of resoles is often referred to as a one-stage process since a quantity of formaldehyde sufficient to permit the formation of highly cross-linked material is present from the outset.[6]

Under the conditions of cure it has been reported that the reactions involving the formation of *ortho*,*ortho*-methylene bridges (Equation 1.16) and dimethylene ether bridges (DMEB) (Equation 4.6) become important reactions.[12]

The main structures believed to be present in cured resole type phenolic resins are characterised by phenolic rings bound by methylene linkages or dimethylene ether bridges (DMEB) with residual methylol groups[13] (Figure 1.2).

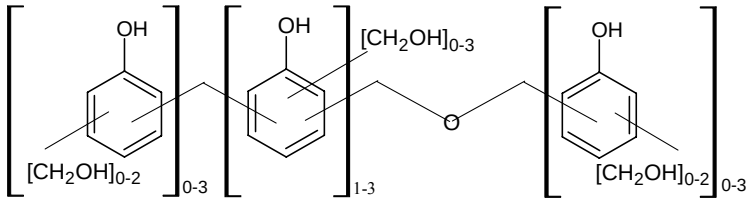

Figure 1.2: A proposed structure of a final cured resole resin.

1.2.3 The Complexity of the Phenolic Resin System

The polymers derived from phenol and formaldehyde differ in one important respect from many other polycondensates, in that phenols are polyfunctional and thus can commonly form a variety of structures for any particular chain length, only differing in their substituents and number thereof (i.e. isomerides). In contrast, the polycondensation products derived from the reaction of amines and alcohols with acids (polyamides and polyesters respectively) in which only one structure for any particular chain length can be formed.[4]

Due to this complexity the polymer chain may not form in a smooth and regular manner which not only makes kinetic studies extremely difficult, but also makes the organic chemistry of the reaction very complex.

The reactions presented above (Equations 1.9 – 1.13) were simplified by considering only the reactions of the monomeric form of formaldehyde. A further simplification was provided by only considering the subsequent reactions of the mono-methylol phenols.

These reactions become immensely more complex when dealing with the various other polymeric forms of formaldehyde (see Section 1.2.1) and the reactions of the dimers and trimers (see Section 4.2)

As well as the numerous reactions possible, a large number of synthesis parameters (i.e. temperature, stoichiometry, pH, catalyst etc.) contribute to the progress of a phenolic resin reaction. These individual parameters affect the reaction pathways possible and hence the final structure and final properties of the resin.

Nuclear Magnetic Resonance spectroscopy (NMR) has previously been shown to be a powerful technique, providing detailed structural analysis of the complex phenolic resin system. NMR has enabled the various isomerides to be unequivocally identified and the effects of synthesis parameters on the final structure to be determined. As a result, NMR is commonly the analytical technique of choice and the dominant analytical technique of the present investigation.

1.3 NUCLEAR MAGNETIC RESONANCE SPECTROSCOPY

1.3.1 Introduction

NMR is a valuable spectroscopic technique due to its ability to identify connections between entities. A variety of weak interactions affect the individual nuclear resonances within a molecule. If these interactions can be disentangled and interpreted, they are found to contain a great amount of information about the structures, conformations and interactions of these molecules.

The theory of NMR is now well established within the literature[14-17]. The following sections introduce the main concepts of NMR, and explain how the technique can be used to gain quantitative information about species present in complex mixtures.

1.3.2 Nuclear Magnetism

When placed in a static magnetic field of flux density (B_0), a single nucleus is said to undergo nuclear magnetic resonance if it possesses an angular momentum (p) (nuclear spin). The spin quantum number, (I) is a constant characteristic of the ground state of every nucleus. Nuclei with $I \neq 0$ interact with magnetic fields due to their magnetic moment (μ). The nuclear angular momentum and the magnetic moment arising from it can be represented as vectors with a constant of proportionality between them, namely the gyromagnetic ratio (γ) (Equation 1.18). It is this constant which determines the resonant frequency of the nucleus.

$$\mu = p\gamma \quad \text{(1.18)}$$

When exposed to a static, homogeneous magnetic field, (B_0) a spinning nucleus behaves like a gyroscope. The spin axis coincides with the magnetic moment vector (μ) which precesses about B_0. The frequency of precession (ν_0) is known as the Larmor frequency of the observed nucleus, and can be calculated (Equation 1.19). From this equation it can be seen that by increasing the field strength we can accelerate this Larmor frequency.

$$\nu_0 = \frac{\gamma}{2\pi} B_0 \quad \text{(1.19)}$$

Nuclei with spin quantum number I may occupy ($2I$+1) different energy levels when placed in a magnetic field. For nuclei with I = ½ e.g. ^{1}H, ^{13}C etc., two spin alignments relative to B_0 arise, these are denoted by +1/2 and -1/2 which correspond to the low energy (i.e. parallel) and high energy (i.e. anti-parallel) alignments respectively, which in turn are separated by an energy difference ΔE (Equation 1.20).

$$\Delta E = E_{-1/2} - E_{+1/2} = 2\mu_0 B_0 = \gamma \frac{h}{2\pi} B_0 \quad \text{(1.20)}$$

At thermal equilibrium the nuclear magnetic energy levels are populated according to a Boltzmann distribution. Therefore a surplus of spins resides in the lower energy level and hence an equilibrium magnetisation (M_0) is built up along the direction of the magnetic field. If we define the z axis of a set of Cartesian coordinates to point along the direction of the magnetic field (B_0), then a single spin has a stationary component of its magnetic moment aligned along the z axis, and a component rotating with its Larmor frequency in the x-y plane (Figure 1.3 (a)). If a magnitude of spins are considered, there are now a surplus of spins aligned with the magnetic field (B_0) in the z direction and hence an equilibrium magnetisation (M_0) (Figure 1.3 (b)).

If a set of coordinates were chosen that rotate with the nuclear precession only the motion of the equilibrium magnetisation (M_0) would be observed. This provides a dramatic simplification of the system and is known as the "rotating frame" of reference (Figure 1.3 (c)).

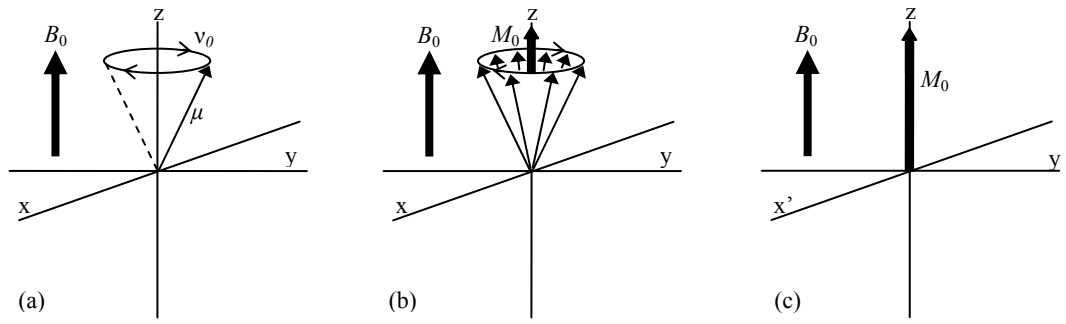

Figure 1.3: (a) The Larmor precession of a single nucleus. (b) The excess low energy nuclei in a sample using standard Cartesian axis, and (c) the excess low energy nuclei viewed from the rotating frame of reference.

1.3.3 A "Pulse"

Application of a tuned radio frequency (r.f.) pulse (essentially an oscillating magnetic field (B_1)) to a sample situated within the static magnetic field (B_0), allows energy absorption (ΔE) to occur, causing these spin states to flip (i.e. resonate).

The sample magnetisation is correspondingly driven around the B_1 field vector (i.e. around the x axis), and in theory can be stopped at any point throughout this rotation, if stopped precisely at the y axis a 90º or π/2 pulse would have been applied (Figure 1.4).

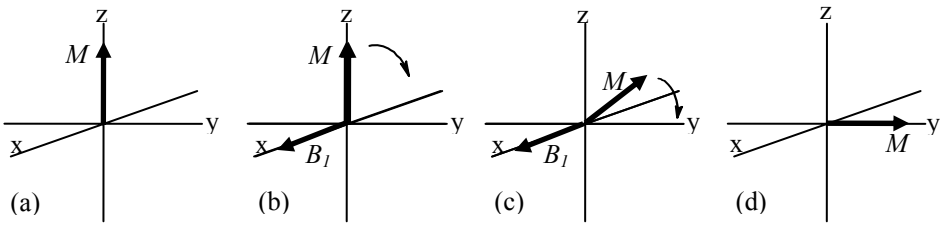

Figure 1.4: A pulse: (a) equilibrium magnetisation, (b) application of a pulse of r.f. radiation perpendicular to the static field, (c) the sample magnetisation being driven around the x axis, and (d) the position of the sample magnetisation after a π/2 pulse

All other pulse lengths leave some of the sample magnetisation along the z axis, where no signal can be generated, and hence a 90º (π/2) pulse generates a maximum signal. In general terms, after a pulse, of angle θ, the component of the magnetisation in the z direction (M_z) is thus given by Equation 1.21:

$$M_z = M_0 \cos\theta \quad \text{..... (1.21)}$$

1.3.4 Relaxation

At resonance the equilibrium distribution of the spins in the static field (B_0) is disturbed. Following any disruption, the nuclear spins relax back to be in equilibrium with their surroundings. Hence the magnetisation reappears along the z axis exponentially (Bloch theory), with time constant T_1, known as the longitudinal (or spin-lattice) relaxation time (Equation 1.22). It is this relaxation that we are observing during the so-called Free Induction Decay (FID) period.

$$M_z = M_0(1 - e^{-t/T_1}) \quad \text{..... (1.22)}$$

Transition energies involved in NMR are so small that in many circumstances the timescale for attaining thermal equilibrium between levels can be very long. This places considerable restraints on the way in which experiments can be carried out.

1.3.5 The NMR Experiment

A sample is subjected to a short burst of r.f. radiation stimulating all signals within the analyte causing them to resonate; this response fades over a period of time. This is analogous in concept to the sound of a struck tuning fork, and can be observed as the Free Induction Decay (FID) signal (Figure 1.5 (a)). Subsequently the experiment can be repeated a number of times, accumulating and summing individual FID's, to increase the signal to noise ratio. When sufficient repetitions have been made, the data are converted from a signal acquired in the time domain signal (FID) to one in a frequency domain signal using a mathematical process known as the Fourier transform (FT). This frequency domain form of the signal constitutes the familiar NMR spectrum (Figure 1.5 (b)).

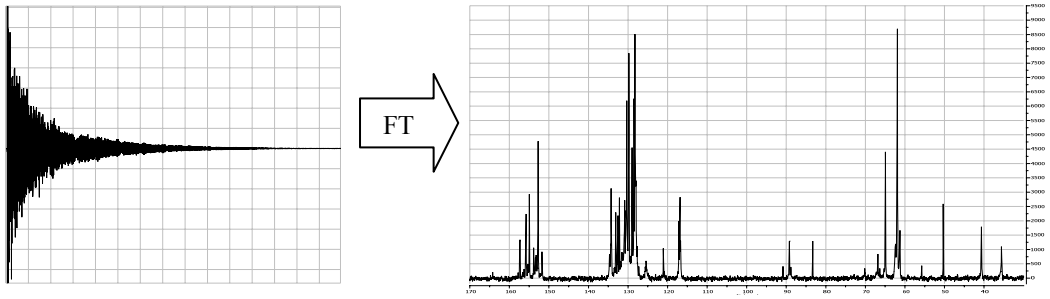

(a) (b)

Figure 1.5: The Fourier transformation (FT) from FID (a) to an NMR spectrum (^{13}C NMR) (b)

1.3.6 NMR Spectra

Within any given molecule several different "chemical environments" exist whereby the outer electron clouds of individual atoms are of differing shape and density, which have small influences on the magnetic field at the nucleus.

The differences in the nuclear precession frequency that these slight changes in environment cause are called the chemical shifts. Instead of a single Larmor frequency for a given NMR active nucleus there is a characteristic spectrum of discrete frequencies (i.e. Figure 1.5 (b)).

The chemical shift at which a nucleus resonates is therefore proportional to the effective magnetic field experienced by that nucleus. Coupling is a consequence of the magnetic interaction between nuclei with spin, this interaction may shield or deshield the nucleus from the external magnetic field. The NMR signal of a nucleus coupled to n equivalent nuclei with spin I will thus be split into a multiplet. The number of resonances observed in the NMR spectrum follows the multiplicity rule ($2nI + 1$), with relative intensities described by Pascal's triangle.

Carbon-13 NMR

The main difficulty in carbon-13 (^{13}C) NMR is the low natural abundance of the ^{13}C nucleus (1.108 %) and its low gyromagnetic ratio (γ) and hence ^{13}C NMR is much less sensitive (1.59%) than ^{1}H NMR (100%).[15]

In many ^{13}C NMR experiments, it is necessary to eliminate the coupling between these nuclei completely, effectively collapsing multiplet signals into discrete single resonances, resulting in a dramatic increase in signal intensity. Decoupling results from the application of an r.f. field exactly at the resonance frequency of one nucleus (e.g. ^{1}H) while observing the NMR spectrum of the nuclei which are coupled to it (e.g. ^{13}C). The result is the proton-decoupled ^{13}C-NMR spectrum which shows the individual carbon atoms as single resonances.

Generally, due to time restrictions, routine NMR analyses are carried out under qualitative conditions allowing intricate structural details of the analyte to be revealed. While quantitative ^{13}C NMR analyses are possible, substantial difficulties remain in selecting the correct experimental conditions to perform the highly precise analysis. The two phenomena that determine how quantitative experiments can be preformed are the relaxation time (T_1) and the NOE factor (see Section 3.7.2 and 3.8.2 respectively).

1.4 NMR STUDIES OF PHENOLIC RESINS

In the past, formulations for phenolic resins have been developed almost entirely on an empirical basis. Complete chemical analysis proves to be extremely difficult due to the complexity and instability of the resin system and hence the immediate requirements of industry were satisfied with little fundamental research.

Improved analytical techniques have allowed for the investigation and identification of phenolic resin species present within a reaction mixture. Thus allowing correlations between the properties of the resins (or resin products) and these species to be made.

Scoping the literature reveals the numerous techniques which are commonly employed to characterise the diverse range of phenolic resins i.e. High performance liquid chromatography (HPLC),[18, 19] gel permeation chromatography (GPC),[18, 20] Fourier transform infrared spectroscopy (FT-IR),[21, 22] matrix assisted laser desorption ionisation time of flight mass spectrometry (MALDI-TOF MS),[23, 24] etc. However the analytical technique of fundamental importance, due to its great structure resolving properties, and hence forms the basis of the current investigation is that of ^{13}C NMR.

de Breet et al.[25] published the first study dealing specifically with the ^{13}C NMR analysis of phenol formaldehyde resins. Up until this point, NMR studies of phenolic resins had been limited to those of ^{1}H NMR. Spectra obtained from ^{1}H NMR analyses of phenolic resins were commonly swamped with overlapping signals giving rise to less reliable interpretations. The great success of ^{13}C NMR spectropscopy is due to its much greater spectral window (twenty times that of ^{1}H) and the possible acquisition of decoupled spectra providing a significant simplification of the resulting phenolic resin spectrum. This has allowed de Breet et al. to interpret the phenolic resin spectra with the aid of reference compounds and simple additivity calculations.

It is important to note however that chemical shift assignments based on conventional additivity rules were found to deviate significantly from those observed within sterically crowded systems, as common within phenolic resins. A more accurate means of predicting chemical shifts values of actual phenolic resin species was thus necessary.

Kim et al.[26] reported a large study on the model compounds of simple phenol molecules and provided an alternative method for predicting chemical shift values. The variation in chemical shift values for the individual model compounds were monitored (via ^{13}C NMR) under a series of solvent conditions, comparable to those employed during a commercial phenolic resin synthesis. Upon analysis of a commercial type phenolic resin, the chemical shift assignments made, although based on those of model compounds, were now more comparable to those observed, due to the solvent-solute interactions present.

Following the pioneering investigations of de Breet and Kim, many studies have reported the use of ^{13}C NMR as a technique to characterise and determine the effects of varying reaction parameters on the structure of the final resin i.e. formaldehyde/phenol molar ratios (F:P),[27, 28] catalyst,[27-29] and alkalinity.[30] However, reliable comparisons between studies, where phenolic resins are produced under a number of different reaction conditions is a difficult exercise and must be approached with care.

The knowledge of the chemical structure of phenolic resins, based upon characterisation of the final condensation product proves to be greatly valuable. However further advancement can readily be obtained from an investigation of the reactions leading up to this final condensation product, rather than after the synthesis has taken place.

For instance, after proposing supplementary chemical shift assignments and various amendments to those available, Werstler[31] presented the first attempt to fully quantify a phenolic resin reaction by NMR. This advance was possible due to the strictly defined NMR conditions and the knowledge of phenolic resin relaxation times and NOE factors (see Chapter 3).

This allowed Werstler to effectively carry out a phenolic resin reaction (14 days and at room temperature) and monitor the structural changes during a resin synthesis via NMR.

Further improvements of the ^{13}C NMR technique allowed for more comprehensive and detailed studies of the reactions involved in a phenolic resin synthesis to be carried out.

Kim et al.[32] provided a method of reaction monitoring, whereby ten intermediate samples were taken during a commercial type phenolic resin reaction. These samples were then analysed under quantitative NMR conditions, by coupling this NMR data with complementary data obtained from GPC allowed the authors to calculate apparent kinetic parameters. The NMR spectra recorded at the various stages of reaction allowed also for the prediction of an average resin structure.

Monni et al.[33] studied a phenolic resin reaction, where the only reaction condition changing was the degree of condensation. ^{13}C NMR provided structural information at various stages throughout the reaction, while a host of physical techniques (i.e. viscosity, GPC, etc.) allowed correlations between resin structure and physical properties of the resin to be drawn.

In practice these experiments afford information about the final resin and only a limited number of stages of the reaction. The advancement of *in situ* monitoring of phenolic type reactions has been published in two interesting papers. Although not focussed directly on resole type phenolic resins these reports provide great insight into the possibility of "real time" reaction monitoring.

The first, a paper presented by Sojka et al.[34] involved the *in situ* monitoring of the reaction between phenol and hexamethylenetetramine. In this investigation the reactants were added directly into an NMR tube and the reaction commenced inside the NMR spectrometer. This *in situ* technique allowed changes in the reaction mixture to be monitored as changes in the sequential NMR spectra acquired, as a function of time.

The second reported work in this area appears five years after the Sojka paper, where an *in situ* ^{13}C NMR study into the reaction of Novolak type phenolic resins was presented by Pethrick et al.[35] Similarly sequential spectra could be obtained allowing the authors to identify mechanistic features associated with novolac formation.

The major advancement of these *in situ* methods were the sequential spectra available, which allowed intricate details of this reaction to be revealed i.e. the consumption of reactants, identification and monitoring of subsequent intermediates, and the formation of products.

The above two reports provided the authors with a means to construct profiles of reaction progress as a function of time (i.e. reaction profiles), and hence allow for mechanistic details to be proposed. However, in both of these reports the *in situ* reactions were carried out under isothermal conditions, rarely the case in commercial synthesis furthermore the data obtained could not be quantified, an essential component for meaningful kinetic studies.

A need is therefore apparent if quantitative *in situ* reaction monitoring is to be advanced under industrial conditions. The ability to monitor the reaction in real time and provide quantitative data on reaction intermediates would allow reaction pathways to be investigated.

A significant advancement into the quantitative *in situ* monitoring of urea formaldehyde resins was presented by Zeng.[10] In this research a novel NMR acquisition method was developed whereby real time qualitative spectral data, obtained during an *in situ* resin synthesis, were converted into quantitative data. The conditions of this synthesis were closely related to those applied in industry and hence provided data representative of the commercial process.

This advancement not only allowed for quantitative reaction profiles to be obtained, but allowed the concentrations of individual chemical species to be continuously monitored and hence kinetic studies to be conducted.

The NMR spectra obtained at specific time intervals during the synthesis, corresponded to essentially snapshots of the reactions progress. By having precise control over the reaction conditions Zeng was able to investigate a variety of reaction parameters (e.g. temperature, stoichiometry, pH etc.) and monitor the effects structurally, eventually leading to the proposal of optimum reaction conditions for the urea formaldehyde reaction.

For the present investigation it was proposed that Zeng's technique should be applicable to the analysis of phenolic resins. However, because of the poly-functionality of phenol, the phenolic resin system can be expected to give much more complex NMR spectra. Thus significant preliminary work to establish appropriate parameters and conditions was anticipated.

1.5 SPECIFIC OBJECTIVES – SCOPE OF THE PRESENT INVESTIGATION

A major goal of the present investigation was to take the methods previously applied by Zeng and develop them further for the analysis of phenol formaldehyde resin adhesives. Several questions needed to be addressed.

1. Is it possible to develop this method further for new resin systems and in particular the phenolic resin system? Or was this method specific to the analysis of urea formaldehyde resins?

2. What are the main parameters that need to be taken into consideration when adopting this method for new resin systems?

Although these NMR methods are based on those of Zeng's the individual NMR parameters employed differ significantly due to the difference in resin system under investigation. Hence prior to investigative work these parameters need to be explored.

Another principal goal of this project was to investigate the transient species and reaction products generated during and monitor their concentration changes throughout a commercial phenolic resin preparation. Thus, in brief the specific objectives of this thesis were to report the following:

- The development of a high resolution ^{13}C NMR method capable of identifying the species present and monitoring their concentration during the preparation of phenol formaldehyde resins.

- The application of the method to monitor the reactions taking place in a phenolic resin reaction carried out under conditions similar to those used in an industrial process

This project will help form the basis for further work, to provide new information about how to optimise adhesives that are supplied to the Plywood and LVL industries. Extension of this work will allow the effects of varying synthesis parameters to be determined and hence optimisation of reaction conditions. Thus the long term goal term goal of these investigations is to develop new, more innovative and cost-effective resins.

1.6 STRUCTURE OF THE THESIS

Chapter 1 is an introduction to the topic and includes brief accounts of the chemistry of phenolic resin reactions, and the basic NMR theory necessary to understand the development of the *in situ* (Rapid) monitoring method. Chapter 2 covers the methods and materials used in the work including details of the NMR experiment, the additional analytical techniques investigated and the preparation of phenolic resin. In Chapter 3 the rapid method is developed where key parameters are obtained and finally applied to the analysis of an *in situ* phenolic resin reaction. Chapter 4 is concerned with the investigation of a commercial type phenol formaldehyde reaction in real time and provides quantitative data on transient concentrations as the reaction proceeds, and discusses these results in terms of possible mechanisms. Chapter 5 is a general discussion of what has been achieved and outlines how the rapid method might be developed further to optimise industrial polymerisations.

2 Materials and Methods

2.1 NUCLEAR MAGNETIC RESONANCE SPECTROSCOPY

2.1.1 General NMR Conditions

NMR spectra were acquired using a 10 mm multinuclear probehead installed on a Bruker Avance DRX 300 Fourier Transform spectrometer, operating at 300.13 MHz for proton and 75.47 MHz for carbon.

Unless otherwise stated, NMR spectra were recorded at 308 K (35ºC), using proton decoupling. Chemical shifts are reported relative to the acetic acid carbonyl peak (CH_3**C**OOH) of the internal solvent resonating at 178.99 ppm. Free induction decay (FID) signals were processed either online using Bruker TopSpin software (version 1.3, Bruker BioSpin 2005) or offline using MestReNova software (version 5.0.3-2414/2716, 2007 Mestrelab Research S.L.).

An internal tube arranged coaxially (Figure 2.1), containing a mixture of deuterated (200 µL, CD_3COOD; Acetic-d_3 Acid-*d*, 99.5% atom % D, Aldrich, Milwaukee, WI) and non-deuterated glacial acetic acid (300 µL, CH_3COOH, Ajax Analar Reagent) provided adequate deuterium lock and integration reference.

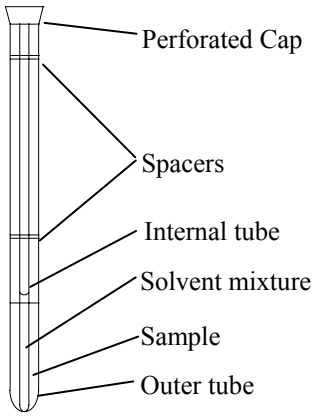

Figure 2.1: The coaxial arrangement of the sample and solvent tubes used for the NMR analyses of the present investigation.

2.1.2 Acquisition Methods

Two NMR data acquisition methods were utilised throughout this investigation, depicted as "The Quantitative Method" and "The Rapid Method". The two methods differ significantly in the way in which spectra are obtained; the most notable differences being the acquisition time and pulse repetition rates.

A table of the typical acquisition conditions for the two NMR methods used throughout this investigation is presented below (Table 2.1):

Table 2.1: Typical NMR acquisition conditions for the Quantitative and Rapid NMR methods.

Parameter	Quantitative	Rapid
Pulse angle	π/2	π/2
Number of FID points	32 K	32 K
Repetition delay (D_1)	40 s	0.6 s
Decoupling mode	Inverse gated	Power gated
NOE enhancement	No	Yes
Number of scans	128	32
Typical acquisition time	1.30 h	1.48 s
Analysis temperature	308 K	Variable
FID Acquisition time (AQ)	0.904 s	0.904 s
Receiver gain	8192	8192

The two NMR methods provide two independent spectral data sets. Details of how the pulse programs differ and how the spectral data derived from these methods differ are explained in further detail below:

2.1.3 The Quantitative NMR Acquisition Method

The pulse sequence employed in the Quantitative method is depicted in Figure 2.2 below:

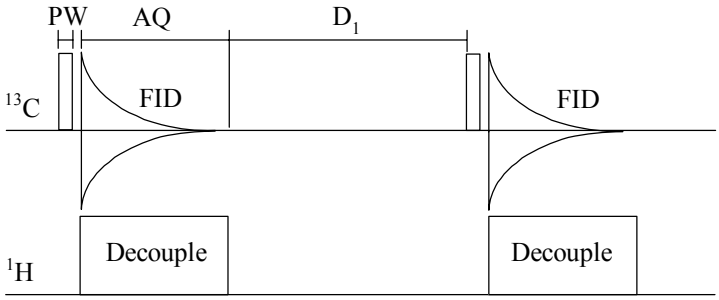

Figure 2.2: Schematic representation of the pulse program used in "Quantitative" experiments

The ^{13}C channel of the Quantitative NMR pulse program follows the sequence: pulse (PW), acquisition (AQ), pulse delay (D_1), followed by the desired number of repetitions.

WALTZ modulated ^{1}H broadband decoupling is only gated on during the acquisition period. This technique is used to suppress additional (and in this case unwanted) enhancements due to NOE (see Section 2.1.4) and is commonly known as inverse gated decoupling.

Inverse gated decoupling saturates the signals arising from the protons within the sample effectively eliminating ^{1}H–^{13}C couplings providing decoupled spectra with quantitative intensities, if appropriate delays are employed (see Section 3.2).

2.1.4 The Rapid NMR Acquisition Method

The pulse sequence employed in the Rapid method is depicted in Figure 2.3 below:

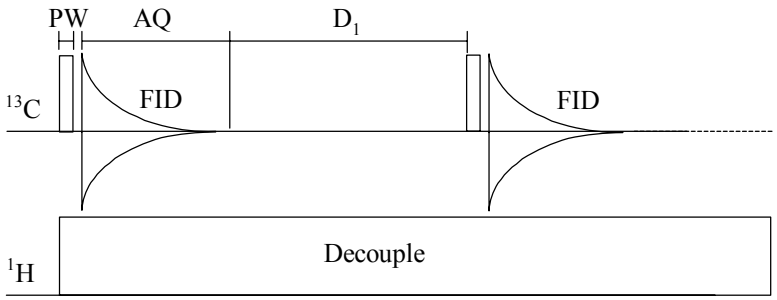

Figure 2.3: Schematic representation of the pulse program used in "Rapid" experiments

The ^{13}C channel of the Rapid NMR pulse program follows the same sequence of events as the quantitative method, i.e. pulse (PW), acquisition (AQ), pulse delay (D_1), followed by the desired number of repetitions. However the interpulse delay is much shorter than the quantitative method

A further major difference between the two pulse sequences is that in the rapid procedure the ^{1}H channel is gated on throughout the entire experiment. This technique is known as broadband or power gated decoupling.

The continuous application of ^{1}H decoupling leads to protonated carbons experiencing a significant enhancement, the Nuclear Overhauser Enhancement (NOE), hence spectra obtained using the rapid method are qualitative and have difference intensities.

2.1.5 Temperature Control

When scaling the reaction down to NMR dimensions problems were encountered due to the crude temperature monitoring of the NMR spectrometer. The variable temperature unit (VTU, Bruker) of the NMR spectrometer was found to be in error and was systematically overshooting the intended set temperature.

To probe the extent of the true temperature deviation from that set, an alternative strategy was devised to measure the true temperature inside the spectrometer probe. A series of heating experiments were carried out whereby the VTU was set at a specific temperature and after an equilibration period the temperature inside the spectrometer probe was measured using a long thin thermocouple situated within a sample tube (CHY502 K/J Thermometer and thermocouple wire).

2.1.6 Additional NMR Investigations

DEPT-135

Distortionless Enhancement by Polarisation Transfer (DEPT-135) spectra were obtained to discriminate between the various carbon atoms within a phenolic resin sample. Quaternary carbons are suppressed while methine and methyl carbons (CH and CH_3) have positive intensities and methylene carbons (CH_2) have negative intensities. DEPT-135 spectra were acquired with a D_2 value of 0.038 s and processed as previously described (Section 2.1.1).

2D NMR

2D COSY, HMBC and both long range and short range HSQC-TOCSY spectra were acquired using a 5 mm inverse probehead (optimised for ^1H detection) installed on a Bruker Avance DRX 400 Fourier Transform spectrometer, operating at 400.13 MHz for proton and 100.61 MHz for carbon. The resulting FID's were processed using the same software previously described (see Section 2.1.1)

2.2 ADDITIONAL TECHNIQUES INVESTIGATED

2.2.1 Infrared Spectroscopy

Two Infrared (IR) methods were investigated for the analysis of phenolic resin adhesives; they were as surface films and Attenuated Total Reflection Infrared Spectroscopy (ATR-IR) a described below:

ATR-IR spectra were recorded using a Thermo Spectra-Tech ATR cell, utilising a ZnSe multi-pass crystal. The phenolic resin samples of interest were smeared across the entire length of the ATR crystal without further preparation and the analysis carried out.

Phenolic resin samples were also analysed, without further preparation, as surface films between calcium fluoride (CaF_2) windows using a press lock cell.

All Infrared spectra were recorded at room temperature on a DigiLab FTS-40 spectrometer, in absorbance mode, with 50 scans per sample. The resulting FT-IR spectra were processed using Win IR software (version 4.14 level II).

2.2.2 Electrospray Ionisation Mass Spectrometry

Electrospray ionisation mass spectra (ES-MS) were determined in positive ion mode (cone voltage: 60 V, cone temperature: 60^{o}C) using a VG Platform II instrument (Fisions Instruments), supported with a Dionex P690 HPLC pump (flowrate 0.02 mL min^{-1}). All spectra were processed using MassLynx software (version 2, 1993).

The resin samples of interest (ca. 50 mg) were dissolved in 1-2 mL of solvent (methanol:distilled water (1:1)) and centrifuged to remove any particular matter, prior to injection and subsequent analysis.

2.3 THE PREPARATION OF PHENOL FORMALDEHYDE RESINS

Due to the commercial sensitivity of this work; the discrete reaction conditions, details about the temperature profiles employed and the specific volumes of reactants used could not revealed.

Several methods for the preparation of phenol formaldehyde resins were utilised throughout this research. Each of the methods provided additional information about the complex reaction under investigation.

In an industrial environment the progress of a phenolic resin reaction is generally monitored as changes in viscosity over time. However, when conducting real time NMR experiments it would be practically difficult to monitor the viscosity due to the small reaction volume and the position of the reaction mixture to be sampled (i.e. within the NMR spectrometer). To address this problem a series of time allocations, corresponding to previous knowledge of viscosity measurements, were utilised throughout this project.

Descriptions of the methods used to prepare phenolic resins as used throughout the current investigation are presented in Sections 2.5.1 – 2.5.3 below.

2.3.1 Preliminary Resin Synthesis

The preliminary resin syntheses were designed to provide resin samples as a function of time (i.e. reaction progress), which could then be used to examine and adjust the spectrometer parameters (those derived in Section 3.2.).

Analysis of these sub-samples provided spectral data as a function of reaction progress and hence provided a general overview of the reactions taking place during the resin synthesis.

A precursor material was utilised in these preliminary reactions as it provided a partially polymerised resin mixture that could be easily transported and allow the polymerisation reaction to be continued to completion at a later time.

This precursor material consisted of a mixture of low molecular weight of methylol phenols.

Preparation of the Preliminary Resin

The precursor material was added directly to an aqueous formaldehyde solution (12.5% w/w) situated within a five necked 1 L round bottom flask fitted with an overhead stirring apparatus (IKA, RW 20 digital), condenser, and a custom temperature control unit which consisted of a thermocouple probe, cooling coil and heating mantle. Stirring was maintained throughout the polymerisation process. The reaction mixture was subjected to a series of predetermined temperature ramps and holds, typically in the range 60 – 97ºC, followed by caustic (46% w/w NaOH aqueous solution) and urea (prills) additions.

2.3.2 Commercial Resin Synthesis on a Laboratory Scale

Once the appropriate NMR parameters had been identified, a representative commercial laboratory scale resin was prepared with an initial formaldehyde/phenol ratio (F:P) of 2.2 and caustic (NaOH)/phenol ratio (C:P) of 0.8.

This reaction mixture was used as a control, and it was from this reaction mixture that the appropriate sub-samples were taken, analysed and used for the determination of both the cross calibration and NOE factors (see Section 3.8.1 and 3.8.2 respectively for further details).

Preparation of the Laboratory Scale resin (Control)

Phenol (88% w/w aqueous solution) and warm formaldehyde (30.5% w/w aqueous solution) were added to the five necked 5 L reaction vessel, with attachments as described previously (Section 2.5.1). Stirring was maintained throughout the polymerisation process. The reaction mixture was heated to 45ºC after which the first addition of caustic (46% w/w NaOH aqueous solution) was made. The temperature was increased steadily to 97ºC where the reaction mixture

was held for a predetermined length of time before being subjected to a series of sequential cooling and holding steps. A second caustic addition was subsequently carried out and the reaction temperature maintained. During the final cooling stage an addition of urea (prills) was performed.

Twenty aliquots (5 mL, sub-samples labelled as: s-1 – s-20) were taken throughout this control reaction, each sample withdrawn represents a specific period of time and hence a specific reaction stage, these samples were frozen until analysis was possible to prevent any further reaction.

NMR Procedure for the Laboratory Scale Resin (Control)

The above aliquots were thawed before 2.5 mL was taken and added directly into a 10 mm NMR tube (7" length, 200 MHz, Wilmad LabGlass) without further preparation. The coaxial tube was inserted and perforated cap secured (see Section 2.1.1) before the sample was transferred into the spectrometer, where it was locked and shimmed before the acquisition was initiated.

2.3.3 Resin Synthesis for Real Time Analyses

For the direct real time monitoring, the reaction was scaled down to NMR dimensions, where the entire reaction was carried out inside a 10mm NMR tube situated inside the spectrometer (*in situ*). For this analysis the final reaction volume was less than 3.0 mL (c.f. industrial resin production ~ 16 tonnes).

Preparation of the Resin used in the Real Time Analysis

Formaldehyde (30.5% w/w) and phenol (88% w/w) as aqueous solutions were weighed directly into a 10 mm thin walled NMR tube (as previously described) followed with mixing. Caustic (46% w/w NaOH aqueous solution) was weighed directly into the same tube and mixed until a homogenous solution was obtained. The coaxial tube was inserted and perforated cap secured (see Section 2.1.1).

NMR Procedure for the Real time Analysis

The sample (prepared above) was transferred directly to the pre-tuned spectrometer, where the sample was locked, shimmed, and acquisition commenced.

The reaction mixture was heated at a constant rate, to a final temperature of 97ºC at which it was held for a predetermined period time before being subjected to sequential cooling and holding steps. The NMR reaction tube was then withdrawn from the spectrometer and a second addition of caustic carried out. The NMR tube was subsequently re-inserted into the spectrometer and the reaction (and acquisition) continued. A final withdrawal was made followed with an addition of urea. The sample was re-inserted and data acquisition continued until completion.

3 Development of the Rapid NMR Method.

3.1 INTRODUCTION

In this section the development of the rapid NMR method will be described. Spectrometer parameters, spectral information and calibration factors necessary for application of the method are obtained.

3.2 DEDUCING THE NMR SPECTROMETER PARAMETERS

In pulsed Fourier transform NMR spectroscopy, to generate the maximum signal in the NMR spectrum, it is essential that the r.f. pulses are correctly tuned and the optimum relaxation delays for the sample of interest are employed. Therefore the first step in developing this ^{13}C NMR method was to determine these NMR parameters for the system under investigation.

3.2.1 The ^{13}C Transmitter Pulse

In pulsed NMR the intensity of the detected signals (I) is a sinusoidal functional of the excitation pulse angle (θ) as shown Equation 3.1, where, I_0 is the maximum possible signal intensity obtainable[14].

$$I = I_0 \sin\theta \quad \text{.....} \quad (3.1)$$

A pulse that is exactly adjusted to turn sample magnetisation by 90º about the x axis is called the 90º or $\pi/2$ pulse angle. As the pulse angle is decreased ($\theta < 90º$) the time required for the magnetisation vector to relax back to its equilibrium position is subsequently reduced.

However, since some of the sample magnetisation now resides in the z plane, where no signal can be generated, the observed signal intensity is consequently sacrificed. Thus, use of the optimum pulse angle will afford spectra of the maximum intensity in the shortest period of time.

Determining the Optimum Pulse Angle

In order to derive the optimum pulse angle, a series of experiments were carried out where an aqueous formaldehyde sample was subjected to analysis under three different pulse angles, namely 45º, 70º and 90º (Figure 3.1)

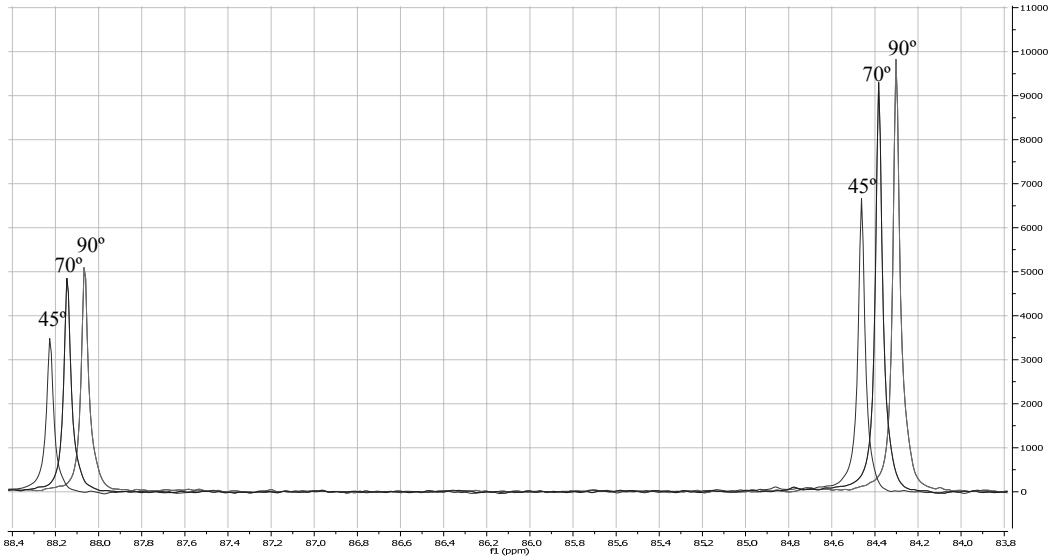

Figure 3.1: Overlapped spectra obtained from the analysis of an aqueous formaldehyde sample with pulse angles 45º, 70º and 90º respectively (N.B. the x axis has been off set for clarity).

As a result of these investigations it was found that although reducing the pulse angle from 90º decreased the acquisition time, the concomitant loss of signal intensity had greater detrimental effects on the analysis. Therefore a pulse angle of 90º was employed in the two pulse programs (see Section 2.1.2) utilised throughout this investigation.

For specific spectrometer probe combinations pulse angles have been calculated as the length in time (usually μs) required for an r.f. pulse to turn the sample magnetisation through the desired angle, which in this study was chosen to be 90º. As the signal intensity, and hence signal-to-noise, depended so strongly on the optimum 90º pulse length, the duration of this pulse length was investigated to ensure the spectrometers pulse parameters were set correctly.

Determining the 90º Transmitter Pulse Length

To deduce the 90º transmitter pulse length, the signal intensity arising from the analysis of an aqueous formaldehyde sample was followed over a range of increasing pulse lengths (2 - 22 μs). Initially a single spectrum was obtained to determine the phase correction required to display a positive absorption spectrum. This was achieved by using a short enough pulse length that corresponded to a pulse angle of less than 90º (i.e. 2 μs). Repeating the experiment with incremental pulse lengths (i.e. 2, 4, 6, . . ., 22 μs) gave rise to a Gaussian type (bell shape) curve (Figure 3.2), rising through a maximum which corresponded to the 90º pulse angle. From this the pulse length giving rise to this maximum can be easily determined.

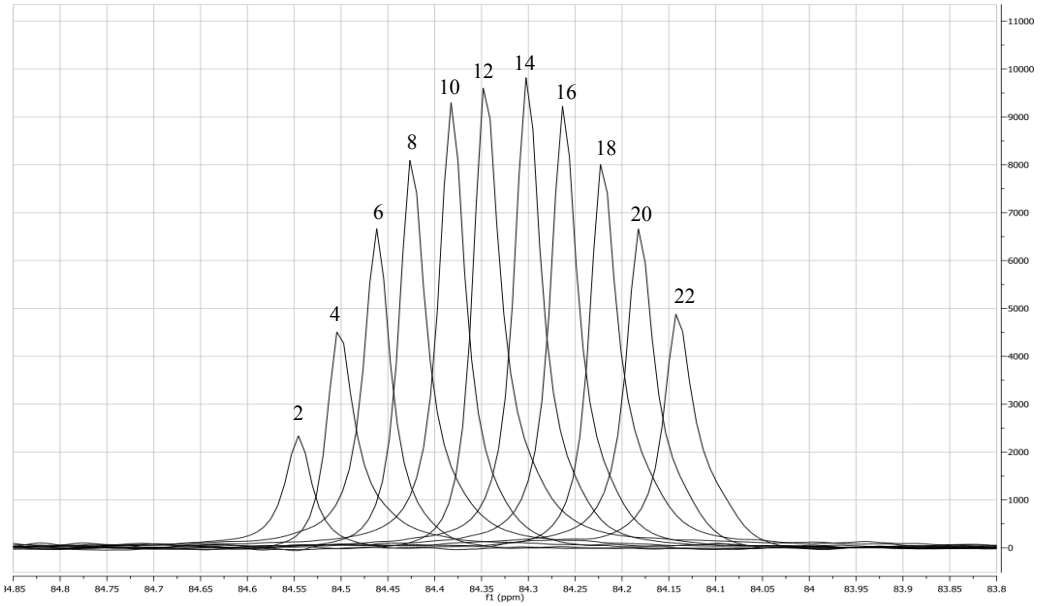

Figure 3.2: Overlapped spectra obtained from the analysis of an aqueous formaldehyde sample showing the changes in signal intensity of the methylene glycol peak, with increasing pulse lengths (μs) (N.B. the x axis has been off set for clarity).

The above described method was however time consuming because of the large number of individual NMR experiments that were required, with each experiment demanding long delays between pulses to ensure complete relaxation. An alternative method exists whereby only two spectra are recorded, hence dramatically reducing analysis time. According to Haupt,[36] if two spectra of the same sample are recorded, where the pulse length of the second is twice that of the first, the 90º pulse angle (θ_1) can be determined according to Equations 3.2 and 3.3. Where I_1 and I_2 are the individual intensities obtained from spectra 1 and 2 respectively.

$$\cos\theta_1 = 0.5\frac{I_2}{I_1} \quad \text{.....} \quad (3.2)$$

$$t_p(90) = \frac{90\, t_{p1}}{\theta_1} \quad \text{.....} \quad (3.3)$$

Using the two pulse lengths, t_{p1} = 6μs and t_{p2} = 12μs (where $t_{p2} = 2t_{p1}$) this method was applied to an aqueous formaldehyde sample (as used previously) resulting in two independent spectra. From the signal intensities arising from the methylene glycol species appearing in both the formaldehyde spectra (I_1 and I_2 respectively) the 90º pulse length ($t_p(90)$) could therefore be calculated.

From this experiment the pulse length $t_p(90)$ was calculated to be 12.6277 μs, in good agreement with the previous method (ca. 13 μs).

In the above set of experiments an overly long delay time had been deliberately chosen to ensure complete relaxation between NMR experiments. This delay time is necessary to produce the *maximum* signal intensity, however the length of this delay obviously restricts how quickly the individual NMR experiments can be repeated. In order to achieve the maximum possible signal in the *shortest* period of time (the goal of most NMR experiments) the optimum repetition rate needs also to be investigated.

3.2.2 Repetition Rate

In pulsed FT NMR, it is common to carry out several NMR experiments (scans) and sum the resulting FID's before Fourier transformation, thus increasing the gain in the signal to noise ratio (*S/N*), according to Equation 3.4, where *NS* = number of scans.

$$S/N = \sqrt{NS} \quad \ldots\ldots (3.4)$$

The steady state NMR signal intensity obtained from a sample following the application of a series of 90º pulses, is however constrained by the need to wait a specific time period between sequential pulses, allowing the recovery of the equilibrium population of aligned and opposed spin states (relaxation), before repeating the NMR experiment.

Following the application of an r.f. pulse, the sample magnetisation reappears along the z axis exponentially, with time constant T_1, known as the longitudinal relaxation time (see Section 1.3). The underestimation of T_1 (i.e. acquiring too rapidly) causes an error in the relative intensity of the species, and overestimation of T_1 (i.e. acquiring more slowly than necessary) causes a loss of signal to noise in a given time. Relaxation times depend on such things as temperature, solution viscosity, molecular size and structure.

The general requirement of a good quantitative NMR measurement is the attainment 99% of the maximum signal intensity. In order to achieve this the repetition rate should typically be of the order of five times the longitudinal relaxation time ($5T_1$) when using a 90º pulse.[16]

In order to obtain a greater understanding of the direct influence of this relaxation time on the analysis of phenolic resin species, and to help deduce the appropriate repetition rates for the two NMR acquisition methods, it was therefore necessary to determine T_1 values for all the major species present in the reaction system under investigation.

The experimental determination of T_1 values for the control phenolic resin reaction, as prepared in this investigation, is reported in Section 3.7.

As a result of these calculations, the individual repetition rates for both the "Rapid" and "Quantitative" NMR acquisition methods were determined (see Table 2.1).

3.3 ^{13}C NMR SIGNAL ASSIGNMENT

The ^{13}C NMR signal assignments of phenolic resin species are reasonably well established in the literature[26, 31, 37-39]. As a result, most of the major signals observed in the present investigation could be assigned using these values. However in some cases known chemical shift additivity rules and DEPT spectra were called upon to assist with these assignments.

Chemical shift assignments based on those obtainable from the literature must be treated with caution, as these values can differ up to 1 ppm depending on the experimental conditions employed (e.g. solvent, temperature, concentration, etc.), and how the chemical shifts were referenced. In this investigation chemical shifts are reported relative to the carbonyl signal of deuterated acetic acid ($CD_3\underline{C}OOD$), as an external standard (see Section 2.1), resonating at 178.99 ppm.

During the synthesis of a phenolic resin, the reaction mixture is subjected to a series of controlled temperature ramps and holds (see Section 2.5). As the temperature of the reaction mixture increases the chemical shift values of all species involved undergo shifts proportional to the increase in temperature. Correlations between the deviations in chemical shift values with changing temperature have been made (see Section 3.4). All chemical shift assignments reported in the present investigation were obtained from spectra acquired at 308 K (35ºC).

Representative spectra of a resin sample (sub-sample, s-6) (Figure 3.2) and a sample of the aqueous formaldehyde solution, as used in this investigation (Figure 3.3) is given below:

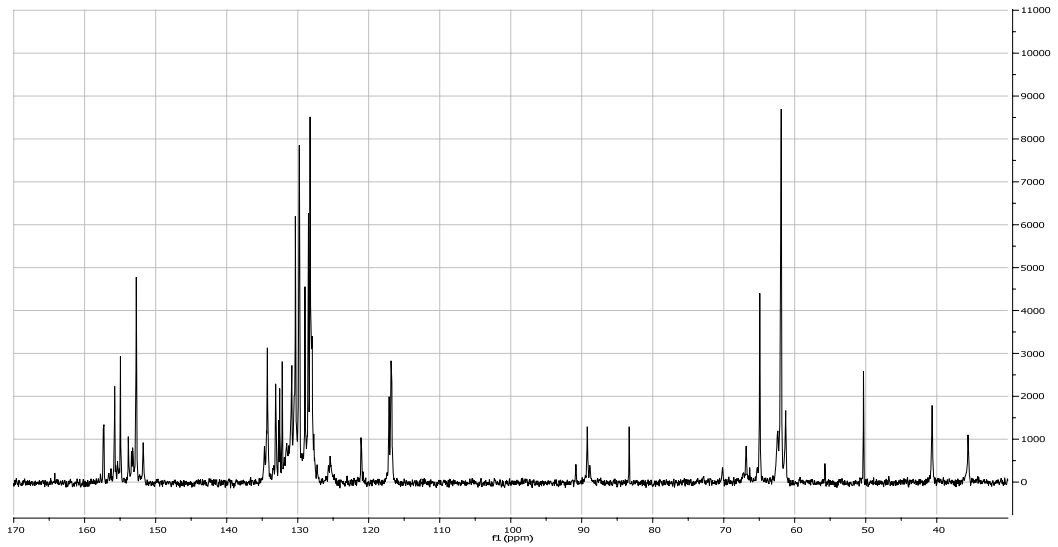

Figure 3.3: A representative ^{13}C NMR spectrum of a phenolic resin sub-sample (s-6) obtained using the "Quantitative" method.

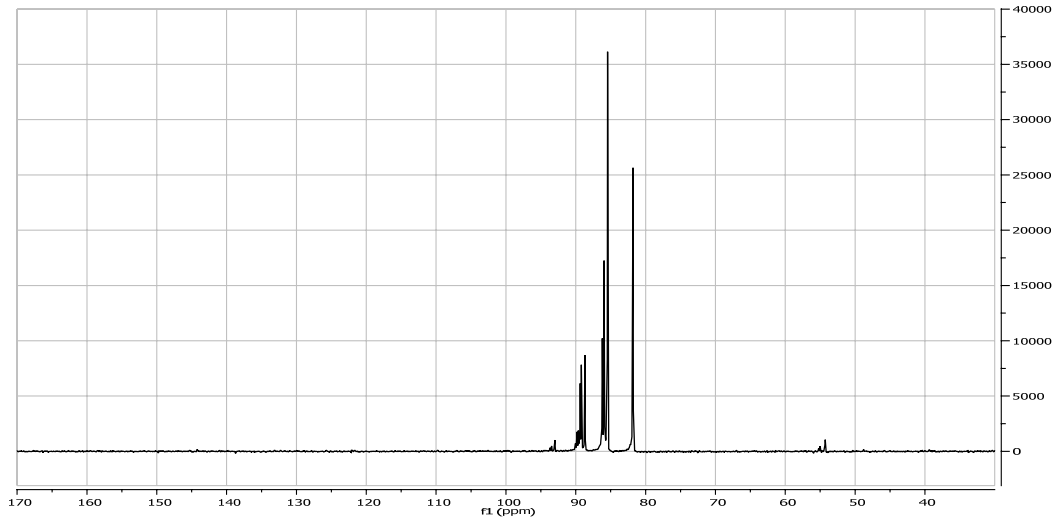

Figure 3.4: A representative spectrum of the aqueous formaldehyde solution as used throughout this present investigation acquired using the "Rapid" method.

Chemical shift assignments of individual species are reported where possible however, some regions in the NMR spectra contain overlapping signals. In such cases chemical shift information from these areas has been reported as ranges. A table of such chemical shift assignments as used throughout the current investigation is given below (Table 3.1).

Table 3.1: A table of the ^{13}C NMR chemical shift assignments, for phenolic resin species, as used throughout the current investigation. (Where Φ represents a phenolic moiety, H – hydrogen atom, MP – methylol phenol, DMP –dimethylol phenol, TMP – trimethylol phenol, PHF – phenolic hemiformal, DPHF – diphenolic hemiformal)

Chemical Shift (ppm)	**Structural Unit**			**Species**
22.75 - 19.50	**C**D_3COOD			deuterated acetic acid - d_4
21.4	**C**H_3COOH			acetic acid
35.6	Φ-**C**H_2-Φ			*ortho,para*-methylene bridge
40.6	Φ-**C**H_2-Φ			*para,para*-methylene bridge
50.5	**C**H_3OH			methanol
55.9	$HOCH_2O$**C**H_3			methoxy carbon of hemiacetal
56.6	$HOCH_2OCH_2O$**C**H_3			methoxy carbon of hemiacetal
56.7	$HOCH_2OCH_2(OCH_2)_nO$**C**H_3			methoxy carbon of long chain hemiacetal
	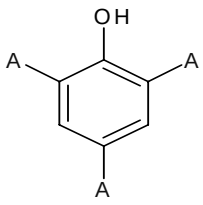			A = H - hydrogen MP - methylol phenol (-CH_2OH) PHF –phenolic hemiformal (-$CH_2O(CH_2O)_nH$)
	2	**4**	**6**	
61.7	**MP**	H	H	2-MP, 2-methylol carbon
62	**MP**	MP	H	2,4-DMP, 2 methylol carbon
62.5	**MP**	MP	**MP**	2,4,6-TMP, 2 methylol carbon
65.2	H	**MP**	H	4-MP, 4-methylol carbon
66.6	**PHF**	H	H	2-PHF, Φ-**C**$H_2O(CH_2O)_nH$
67.2	**PHF**	PHF	H	2,4-DPHF, 2 carbon
70.3	H	**PHF**	H	4-PHF, Φ-**C**$H_2O(CH_2O)_nH$
70.9	PHF	**PHF**	H	2,4-DPHF, 4 carbon

Chemical Shift (ppm)	Structural Unit	Species
83.6	$HO\underline{\mathbf{C}}H_2OH$	methylene glycol
87.3	$HO\underline{\mathbf{C}}H_2O\underline{\mathbf{C}}H_2OH$	dimeric glycol
87.4	$HO\underline{\mathbf{C}}H_2OCH_2OCH_3$	terminal carbon of methoxy
87.7	$HO\underline{\mathbf{C}}H_2OCH_2O\underline{\mathbf{C}}H_2OH$	terminal carbon of glycol
87.9	$HO\underline{\mathbf{C}}H_2OCH_2OCH_2O\underline{\mathbf{C}}H_2OH$	terminal carbon of glycol
88.4	$HO\underline{\mathbf{C}}H_2OCH_2OCH_2OCH_2O\underline{\mathbf{C}}H_2OH$	terminal carbon of glycol
88.9	$\Phi\text{-}CH_2O(\underline{\mathbf{C}}H_2O)_nH$	4-PHF
89.3	$\Phi\text{-}CH_2O(\underline{\mathbf{C}}H_2O)_nH$	2-PHF
90.4	$HOCH_2O\underline{\mathbf{C}}H_2OCH_2OH$	central carbon of glycol
90.6	$HOCH_2O\underline{\mathbf{C}}H_2OCH_2OCH_3$	methylene of methoxy
90.8	$HOCH_2O\underline{\mathbf{C}}H_2O\underline{\mathbf{C}}H_2OCH_2OH$	central carbon of glycol
90.9	$HOCH_2O\underline{\mathbf{C}}H_2OCH_2O\underline{\mathbf{C}}H_2OCH_2OH$	central carbon of glycol
91	$HO\underline{\mathbf{C}}H_2OCH_3$	terminal carbon of methoxy
91.2	$HOCH_2OCH_2O\underline{\mathbf{C}}H_2OCH_2OCH_2OH$	central carbon of long chain
92	$\Phi\text{-}CH_2O(\underline{\mathbf{C}}H_2O)_nH$	2,4-DPHF and variants
93.3	$\Phi\text{-}CH_2OCH_2O(\underline{\mathbf{C}}H_2O)_nH$	2,4-DPHF and variants
94.5	$HOCH_2O\underline{\mathbf{C}}H_2OCH_3$	methylene of hemiacetals
94.9	$HOCH_2OCH_2O\underline{\mathbf{C}}H_2OCH_3$	methylene of hemiacetals
95.1	$H(OCH_2)_nO\underline{\mathbf{C}}H_2OCH_3$	methylene of hemiacetals
118 - 116	C2 and C6	free *ortho* position
122 - 120	C4	free *para* position
128.75 - 124	C2 and C6	bound *ortho*
132 - 128.75	C3 and C5	free *meta*
135.5 - 132	C4	bound *para*
159 - 150	C1	bound *ipso*
180 - 178.5	$CH_3\underline{\mathbf{C}}OOH$	deuterated acetic acid - d_4

A brief description of the specific phenolic resin NMR ranges and the species which give rise to the signals contained within these ranges follows:

"Ipso" Region – 158-150 ppm

Signals in this region arise from quaternary phenoxy carbons, that is a carbon atom of the phenolic ring bound directly to a hydroxyl group. Signals up-field from those of phenol correspond to higher molecular weight products whereby a reaction has taken place at the *ortho* position, signals down-field arise from products where a reaction has taken place at the *para* position.

"Aromatic" Region – 136-116 ppm

Signals in this region arise from the five remaining carbon atoms of the phenolic ring. Due to the various reaction intermediates and products possible this region contains significant peak overlap and hence great complexity. The section representing the most severe overlap (see Figure 3.3) is a combination of signals corresponding to three discrete carbon environments: 1). Carbon atoms at the *para* position of a phenoic ring, bound directly to non-hydrogen substituents (136 – 132 ppm), 2). Un-substituted *meta* carbons of the phenolic ring (132 – 128.75 ppm), and 3). Carbon atoms at the *ortho* position of a phenolic ring bound directly to non-hydrogen substituents (128.75 – 124 ppm). Two distinct groups of signals follow those described above and are those of the un-substituted carbons atoms at the *para* (122 – 120 ppm) and *ortho* (118 – 116 ppm) positions of the phenolic ring.

"Formaldehyde" Region – 96-83 ppm

Peaks in this region arise from the various forms of formaldehyde existing in the reaction mixture. As stated previously (see Section 1.2.1) formaldehyde as an aqueous solution contains very little monomeric formaldehyde (HCOH), typically < 0.1%. Hence signals within this region arise from methylene glycol ($HOCH_2OH$) and its associated polymeric derivatives the hemiformals ($HOCH_2O(CH_2O)_nH$), and the hemiacetals of formaldehyde ($HOCH_2OCH_3$) and their associated polymeric forms ($HOCH_2O(CH_2O)_nOCH_3$).

During later stages of the reaction this region also contains signals from the methylene carbon atoms of phenolic hemiformal species (Φ-$CH_2O(\underline{\mathbf{C}}H_2O)_nH$) (see Section 4.2).

"Phenolic Hemiformal" Region – 71-66 ppm

Two specific sections occur within this region which correspond to *ortho* (68 – 66 ppm) and *para* (71 – 70 ppm) carbon atoms of the phenolic hemiformals. Each section contains two peaks with the upfield signal being assigned to the mono-substituted hemiformal (2 or 4-$\underline{\mathbf{C}}H_2O(CH_2O)_nH$) and the downfield signal assigned to the di-substituted hemiformal (2,4-$\underline{\mathbf{C}}H_2O(CH_2O)_nH$).

"Methylol" Region – 66-61 ppm

Peaks in this region arise from methylol type carbon atoms bound directly to a phenolic ring (Φ-$\underline{\mathbf{C}}H_2OH$). Carbon atoms of methylol groups bound at the *para* and *ortho* positions of a phenolic ring resonate over the regions 66 – 64 ppm and 63 – 61 ppm respectively, depending upon the various other substituents bound to the same phenolic ring.

"Methoxy" region – 57-55 ppm

Three sharp peaks appear in this region and have been assigned to the methoxy carbons of the formaldehyde hemiacetals and their associated polymeric forms ($H(OCH_2)_nO\underline{\mathbf{C}}H_3$).

"Methylene" region – 42-34 ppm

Two distinct signals appear in this region and correspond to those of the *para*, *para*- and *ortho*, *para*-methylene groups, due to the mechanisms available under the conditions of the present investigation the formation of *ortho,ortho*-methylene groups does not occur. The *para*, *para*- and the *ortho*, *para*-methylene groups resonate at 40 – 42 ppm, and 34 – 39 ppm respectively

3.4 CHEMICAL SHIFT VARIATION

Several external influences can have significant effects on the specific chemical shift values of individual resin species (e.g. solvent, alkalinity, temperature etc.) and hence substantial care is required when interpreting spectra over the course of a reaction.

To avoid influences from solvent interactions a coaxial system (see Figure 2.1) has been employed, whereby the lock solvent and reference material are contained within a sealed glass capillary, effectively isolating the sample from these effects. The alkalinity of the reaction mixture has a relatively small influence on the chemical shift values of phenolic resin species and whose effects were masked by those of caused by the variation in temperature, which has the most noticeable influence on these chemical shift assignments.

The effect of temperature on individual chemical shift values was observed by overlapping sequential spectra obtained during an *in situ* reaction at increasing temperature, with a common reference (see Section 3.3) N.B. the intensity of the below signals is changing due to the reaction and not due to temperature effects. (Figure 3.5).

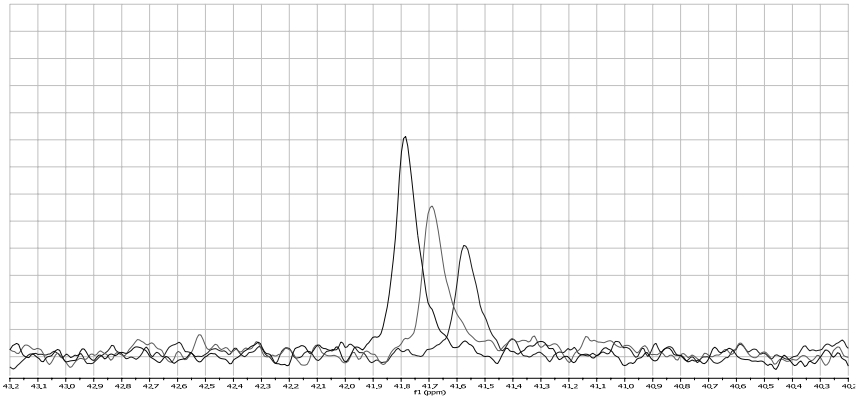

Figure 3.5: The chemical shift variation of the *para*,*para*-methylene bridge species as a function of temperature (spectra number 11, 12, 13).

In order to determine the variation in chemical shift as a function of temperature it was first required to measure the temperature of the sample inside the NMR spectrometer.

The temperature of the NMR spectrometer probe (in which the sample tube is situated) in the present investigation is controlled via a variable temperature unit (VTU). The results of a series of heating experiments (see Section 2.1.5) found that this variable temperature unit was in error and was overestimating the intended set temperature.

The resulting "true" temperatures (i.e. those measured) were plotted against those set by the VTU ("True T" Figure 3.6), and by overlaying a plot the ideal situation, where the measured temperature exactly matches that of the set ("Set T" Figure 3.6) it becomes clear that the true temperature deviates to a greater extent from that set, with increasing temperature.

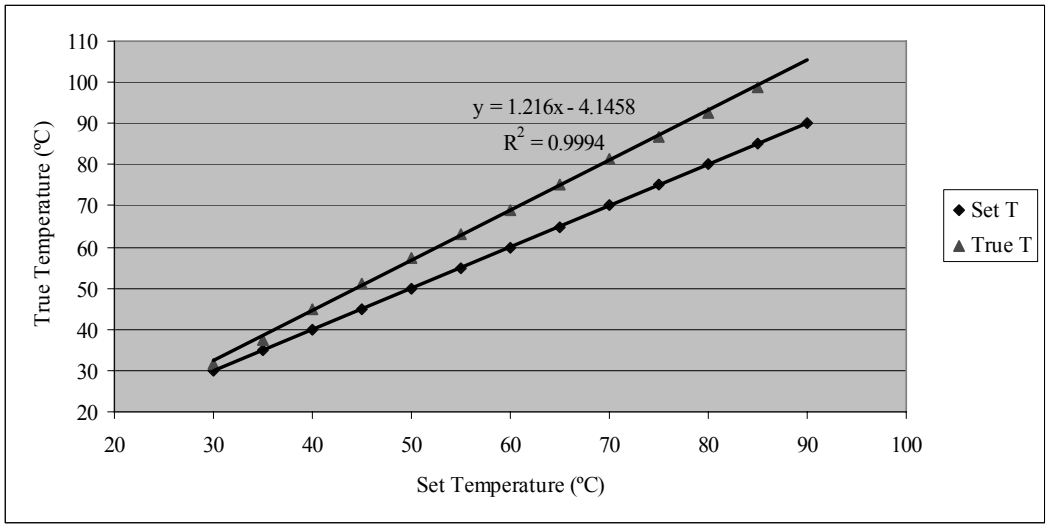

Figure 3.6: A chart showing the increasing error between set and true temperatures

From the slope of the linear "Expt. T" line, the appropriate set temperature could be estimated (i.e. from the relationship: $y = mx + c$) that would give rise to the desired true temperature of the probe. These estimated temperatures were tested to ensure the correct temperature was being applied and were thus employed throughout the *in situ* reactions.

It was found that temperature affected the chemical shift of the reference material linearly and increasing the temperature by 1ºC shifted the chemical shift by approximately 0.3 ppm downfield. This has a substantial effect when trying to monitor discrete integration ranges over the course of a reaction where temperatures can differ by more than 60ºC.

3.5 INTERNAL TUBE AND LOCK SOLVENT/REFERENCE

In this investigation an internal tube arranged coaxially (see Section 2.1) has been used to provide the necessary deuterium lock, chemical shift reference and integration standard. In this section the effect of the internal tubes dimension on the signal intensity has been investigated, along with the process involved in the appropriate selection of NMR solvents.

3.5.1 Internal Tube

In order to determine the optimum inner tube dimension and hence provide the maximum signal while still maintaining adequate lock, several thin walled tubes of differing outside diameters were trialled. A table comparing the internal tube's diameter to resultant volume of the sample has been given below (Table 3.2):

Diameter (mm)	Volume of sample (µl)
5	2000
4	2200
3	2400
2.5	2600

Table 3.2: A table showing the effect of the internal tubes diameter on the sample volume

By increasing the internal tubes dimensions the volume of sample within the analysable region of the NMR probe effectively decreases. However the internal tube provides the lock, reference and integration standard and reducing its volume substantially can have detrimental effects on the analysis. Hence an internal tube with the outside diameter of 4 mm was chosen to allow for sufficient sample volume while maintaining an adequate lock.

3.5.2 Solvent Selection

Samples for NMR analysis are usually dissolved in a deuterated solvent, where deuterium has been used as a lock nucleus. Some factors to be considered when choosing a suitable NMR solvent are: Solubility, interference, temperature dependence, viscosity, cost, and water content. For this work due to the sealed nature of the internal tube, the sample and solvent are effectively partitioned (i.e. isolated from one another). Therefore the solubility, viscosity and water content of the NMR solvent are essentially trivial.

The particular solvent used throughout this investigation needed to fit specific criteria. The solvent itself will inevitably produce NMR signals which will obscure regions of the spectrum, these 'residual solvent peaks' should not overlap with signals from the sample. Since the NMR experiments in this investigation are conducted over a diverse range of temperatures (30 – 97ºC) the solvent's melting and boiling points also need to be taken into consideration.

In order to determine the appropriate solvent for analysis of phenolic resins a review of the common NMR solvents used in the literature was undertaken. This investigation revealed that several of the commonly used NMR solvents are deemed inappropriate almost immediately, when compared to the restrictions placed above e.g. DMSO-d_6 has a boiling point 55ºC and gives rise to a septet centred at 35.9 ppm, directly overlapping with the *ortho*,*para*-methylene signal and hence is an inappropriate NMR solvent, under the conditions of the present investigation.

Conversely deuterated acetic acid (acetic acid-d_4) provides two signals at either end of the phenolic resin spectrum, a singlet at 178.99 ppm and a septet centred at 20.0 ppm. Acetic acid-d_4 has a sufficiently high boiling point (115ºC) and a sufficiently low vapour pressure over the temperature ranges investigated. A low vapour pressure was important so that when the temperature of a sealed tube was increased, there was no risk of the solvents vapour pressure causing pressurisation problems.

The Introducing of non-deuterated acetic acid produces a strong singlet (centred at 20.3 ppm) which provides a more intense (and therefore reliable) integration reference signal. Hence a mixture of deuterated and non-deuterated acetic acid (volumes given previously see Section 2.1) was employed to provide adequate lock and a suitable integration reference.

3.6 DETERMINATION OF THE INTEGRATION RANGES

During the course of the reaction only the simplest products can be identified unequivocally, as certain regions in the NMR spectrum contain significantly overlapping peaks. In addition peaks detected that initially had narrow bandwidth with well defined sharp maxima, become broad over the duration of the experiment.

Therefore an appropriate method of monitoring the reaction's progress that takes into account the challenge of dealing with changing peak shape was necessary. This issue was addressed by performing integration over a region of chemical shift values, thus allowing the change in relative integration areas to be monitored over the course of the reaction.

If an NMR spectrum has been obtained under quantitative conditions the integration area of a specific signal will be directly proportional to the concentration of carbon atoms giving rise to that signal. Therefore changes in the relative integration area of these integration ranges can be essentially viewed as changes in the concentration of species in the reaction mixture.

Two methods for the integration of phenolic resin spectra were trialled: 1). Individual peaks were integrated and summed over the region of interest. 2). Integration ranges were determined that contained all signals of interest within a specific region, i.e. all the polymeric derivatives of methylene glycol (Figure 3.7).

All integration measurements were made relative to the methyl signal of non-deuterated acetic acid (see Section 3.5.2), integrated over the range 22.00 – 19.50 ppm.

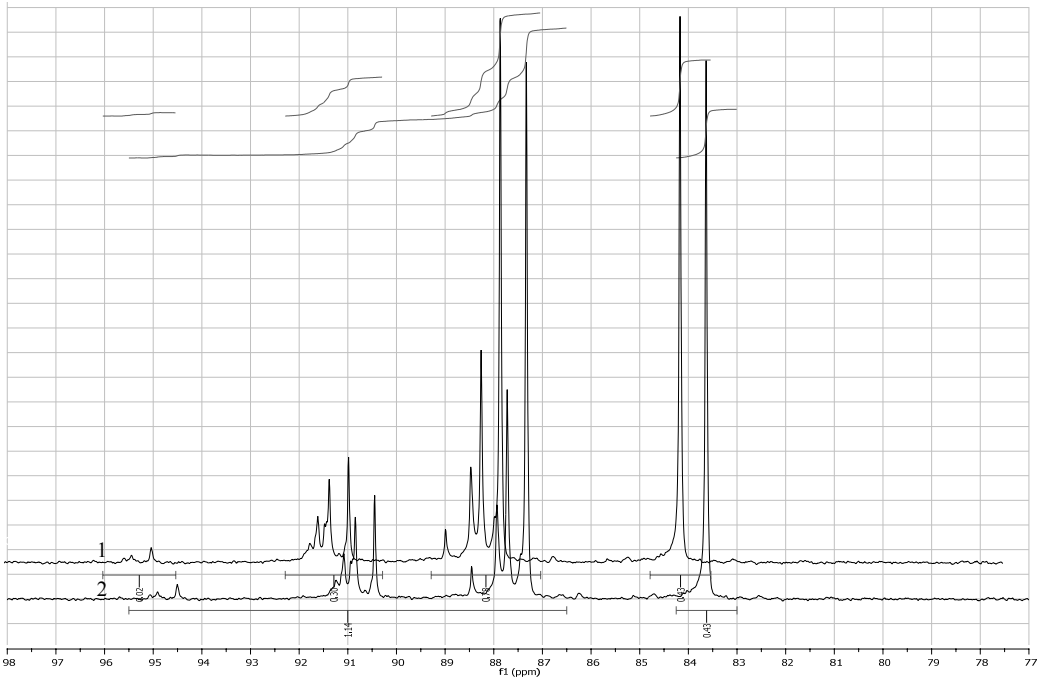

Figure 3.7: The two methods of integration trialled, labelled as1 and 2 respectively.

The first integration method proved to be time consuming due to the large number of individual integration ranges that were required before summation. When the summation of these individual integration ranges were compared to the integration ranges obtained by using the second method (which integrated over whole regions) and applied to several reaction stages, the results were very similar.

Therefore due to its ease of use (less individual integration ranges) and time efficiency the second integration method was utilised throughout this investigation.

18 integration ranges (see Table 3.3) were chosen which incorporated all the major species present throughout a typical phenolic resin reaction.

Table 3.3: A table of the 18 integration ranges used throughout this work at 308K (35ºC).

No.	Integration Range (ppm)	Species
1	22.00 – 19.50	acetic acid (external integration reference)
2	36.65 – 35.90	*ortho*, *para* – methylene bridge
3	41.65 – 40.75	*para*, *para* – methylene bridge
4	50.75 – 50.25	methanol
5	57.00 – 55.50	methoxy carbon of hemiacetal
6	62.00 – 61.50	*ortho* methylol
7	66.00 – 64.75	*para* methylol
8	67.50 – 66.00	*ortho* hemiformal
9	71.45 – 69.85	*para* hemiformal
10	85.45 – 82.00	methylene glycol
11	96.35 – 85.85	Longer chain formaldehyde oligomers
12	118.80 – 115.80	Free *ortho* position of a phenolic ring
13	122.50 – 119.75	Free *para* position of a phenolic ring
14	129.85 – 127.70	Bound *ortho* position of a phenolic ring
15	131.55 – 129.40	Free *meta* position of a phenolic ring
16	135.30 – 131.55	Bound *para* position of a phenolic ring
17	159.25 – 156.05	Bound *ipso* position of a phenolic ring
18	180.00 – 178.75	acetic acid (external chemical shift reference)

By monitoring changes in the integration ranges over time reaction profiles can be obtained and hence the progress of the reaction can be monitored. However, these integration ranges must be used with caution when applying to spectra obtained over a range of temperatures (see Section 3.4).

3.7 LONGITUDINAL RELAXATION TIMES

The observed signal in an NMR spectrum depends on the population difference between the states available to the nuclei under investigation. In order to obtain maximum signal and hence quantitative results, the time between scans must be adequate to allow complete relaxation of the nuclei. This time is generally taken as five times the longitudinal relaxation time (T_1) which is the time constant for re-establishing equilibrium after an r.f. pulse. Therefore, to ensure the condition for quantitative NMR conditions, individual T_1 values for phenolic resin species needed to be calculated.

3.7.1 The Inversion-Recovery Method

The most common technique for determining the longitudinal relaxation time (T_1) is referred to as the inversion-recovery method, and follows the pulse sequence: π, τ, π/2, where τ is the delay time between pulses (Figure 3.8).

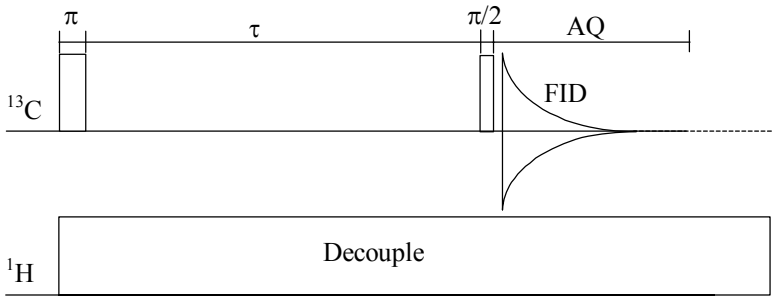

Figure 3.8: A schematic diagram showing the inversion recovery pulse sequence as used to determine individual phenolic resin T_1 values.

In equilibrium nuclei arrange their "spins" to be in the most stable energy state. When these nuclei are introduced into a magnetic field more "spins" are aligned parallel to the magnetic field than those opposed (lower energy state) this is known as the equilibrium magnetisation (M_0) (see Section 1.3).

Starting at equilibrium, applying a π pulse along the x axis inverts this magnetisation vector, i.e. $M_0 \rightarrow -M_0$. By subsequent longitudinal relaxation, the sample magnetization (M_z) returns to its equilibrium position, going from $-M_0$ through zero to $+M_0$, according to the Bloch Equation:

$$\frac{dM_z}{dt} = -\frac{M_z - M_0}{T_1} \quad \ldots\ldots (3.5)$$

Depending on the delay time (τ) between the two pulses, the magnetization has partially relaxed toward the equilibrium position. Following the π pulse, a π/2 pulse is then applied and rotates the partially relaxed magnetization towards the y axis. The resulting transverse magnetisation then relaxes, once again towards equilibrium, giving rise to an FID signal which is then Fourier transformed to give the resulting NMR spectrum.

If the delay time between the two pulses is sufficiently short and hence gives insufficient time for the nuclear spins to re-achieve equilibrium, the majority of the sample magnetisation remains in the –z plane (i.e. $M_z < 0$). Applying a π/2 pulse then flips this magnetisation into the –y plane giving rise to an "inverted" absorption spectrum.

Similar situations can be envisaged whereby increasing the delay time gives rise to a nulled signal (i.e. $M_z = 0$) and a positive absorption spectrum (i.e. $M_z > 0$).

Determining the longitudinal relaxation times can be achieved by integration of the Bloch equation (Equation 3.6) yielding Equation 3.7:

$$\int_{-M_0}^{M_z} \frac{\mathrm{d}M_z}{M_z - M_0} = -\frac{1}{T_1}\int_0^{\tau} \mathrm{d}t \quad \ldots\ldots (3.6)$$

$$\ln\frac{M_0 - M_z}{2M_0} = -\frac{\tau}{T_1} \quad \ldots\ldots (3.7)$$

The signal intensities *I* correspond to the transverse magnetization after the π, τ, π/2 sequence therefore Equation 3.7 can be represented as Equation 3.8 below.

$$\ln \frac{I_\infty - I_\tau}{2I_\infty} = -\frac{\tau}{T_1} \quad \text{..... (3.8)}$$

Here I_τ and I_∞ are signal intensities at pulse interval τ and ∞, respectively. The magnitude of I_∞ can be determined by extrapolating the plot I_τ vs. τ to $\tau = \infty$.

Rearrangement (of Equation 3.8) leads to Equation 3.9:

$$\ln(I_\infty - I_\tau) = [\ln 2 + \ln I_\infty] - \frac{\tau}{T_1} \quad \text{.....…. (3.9)}$$

Therefore a plot of $\ln(I_\infty - I_\tau)$ vs. τ yields a straight line of slope – $1/T_1$

Different T_1 values exist for all the different chemical environments within a molecule and since NMR signal intensities can be greatly affected by T_1 values, it is important that individual relaxation times be determined.

3.7.2 Experimental Determination of Phenolic Resin T_1 Values

The inversion recovery sequence (above) was employed to derive relaxation times for individual phenolic resin species. Four stages throughout the control reaction were analysed (sub-samples s-1, s-5, s -8, and s-20).

35 independent delay times were investigated ranging from $1x10^{-7}$s through to 70s, producing 35 individual spectra per sample, each requiring 32 scans to achieve adequate signal to noise and corresponding to a total analysis time of about 17 hours per sample.

Each series of spectra were phase corrected to show the correct sign, if τ was short relative to T_1 then the signal appeared negative, and if τ was long relative to T_1, the signal appears positive. In between these two extremes the magnitude of the signal intensity increases exponentially through zero with increasing τ (Figure 3.9).

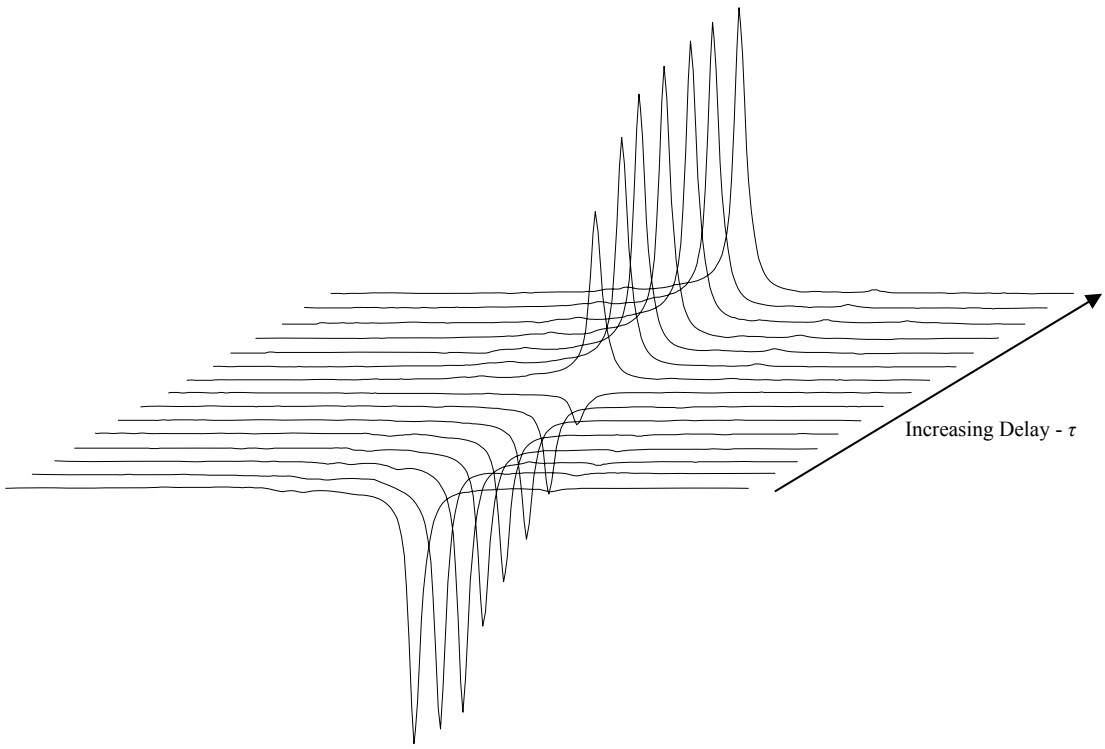

Figure 3.9: A series of stacked spectra for an example signal - the "free" *ortho* signal of phenol, resonating at 121.7 ppm (s-1) showing the effect of the inversion recovery method on signal intensity.

Selected individual signal intensities, obtained from the 35 individual spectra were plotted against their associated delay times (τ). This produced a series of plots showing the exponential increase of signal intensity with increasing delay times for a particular stage of the reaction (Figure 3.10).

The intensities (I_τ) obtained from the exponential region of these plots (i.e. Figure 3.10) were then used to determine the value "$\ln(I_\infty - I_\tau)$" (see Equation 3.9), where I_∞ was taken as the maximum signal intensity observed.

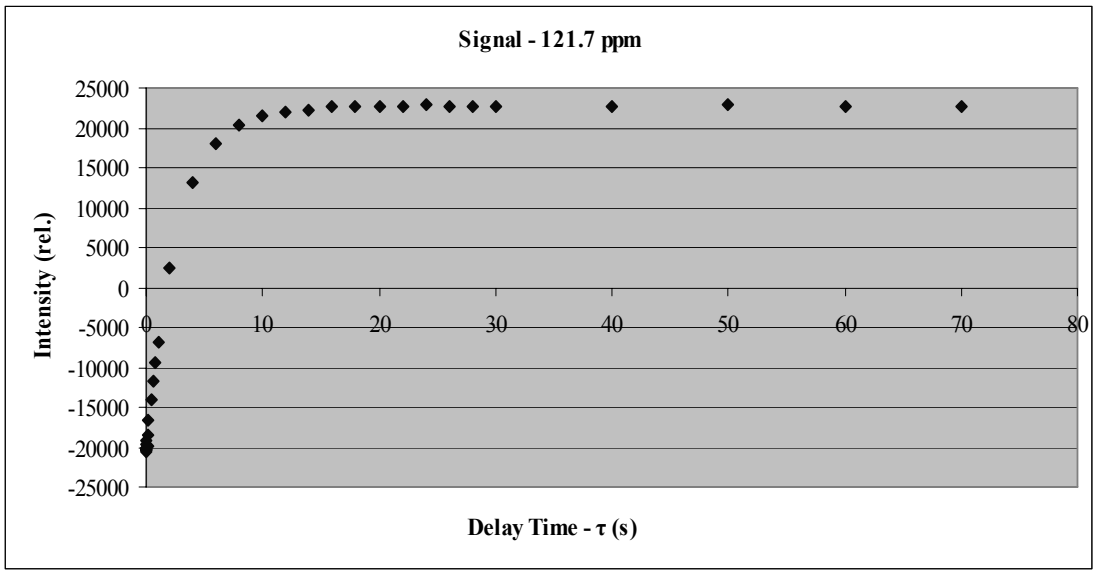

Figure 3.10: A plot of intensity vs. delay time, for the "free" *ortho* signal of phenol resonating at 121.7 ppm obtained from sub-sample s-1.

Table 3.4 shows an example calculation of the "$\ln(I_\infty - I_\tau)$" values from the signal intensity arising from the analysis of the free *ortho* position of the phenolic ring from sub-sample s-1 (via the inversion-recovery method, Figures 3.8 and 3.9).

Table 3.4: Table showing the calculation of the $\ln(I_\infty - I_\tau)$ values from the delay times (τ) and their associated intensities (I_τ).

τ (s)	0.1	1	2	4	6	8	10
I_τ (rel.)	-19782.3	-6968.1	2527.4	13248.9	18074.2	20401.7	21418.8
$[I_\infty - I_\tau]$	42551.3	29737.1	20241.6	9520.1	4694.8	2367.3	1350.2
$\ln[I_\infty - I_\tau]$	10.658	10.300	9.9155	9.1612	8.4542	7.7695	7.2080

The obtained values "ln($I_\infty - I_\tau$)", for the individual integration ranges, were plotted against the delay time (τ) yielding a linear relationship (Figure 3.11).

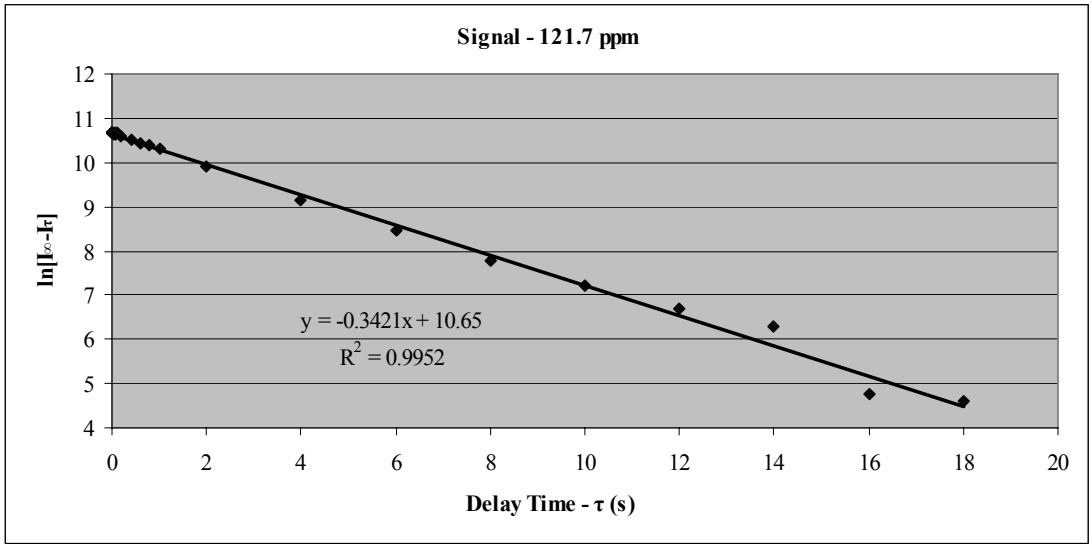

Figure 3.11: A plot of ln (I_∞ - I_τ) vs. delay time, for the "free" *ortho* signal of phenol resonating at 121.7 ppm (s-1)

According to Equation 3.9 the longitudinal relaxation time, T_1, can thus be determined from the slope of this linear relationship ($-1/T_1$).

A T_1 value of 2.92s was obtained for the above example (*ortho* signal of phenol), to achieve complete relaxation and hence for obtaining reliably quantitative spectra (i.e. by using $5T_1$) for this particular signal, an inter-pulse delay time (D_1) of greater than 14.6s is required.

Longitudinal relaxation times were used, not only to determine the appropriate repetition rates of the experiments (see Section 3.2.2), but they also play an important role in deriving the cross calibration factors used for predicting quantitative intensities from non-quantitative spectral data (see Section 3.8).

The following four tables (Tables 3.5 – 3.8) show the phenolic resin relaxation times as determined in the present investigation.

Table 3.5: Relaxation times (T_1) determined from sub-sample s-1

No.	Chemical Shift (ppm)	T_1 (s)	5* T_1 (s)
1	21.39	8.9847	44.9236
2	-	-	-
3	-	-	-
4	50.56	12.7226	63.6132
5	55.89	10.2987	51.4933
6	-	-	-
7	-	-	-
8	-	-	-
9	-	-	-
10	83.61	4.9044	24.5218
11	-	-	-
12	116.65	3.9216	19.6078
13	121.71	2.9231	14.6156
14	-	-	-
15	130.99	4.0016	20.0080
16	-	-	-
17	156.91	4.2553	21.2766
18	178.99	25.8398	129.1990

Table 3.6: Relaxation times (T_1) determined from sub-sample s-5

No.	Chemical Shift (ppm)	T_1 (s)	5* T_1 (s)
1	21.41	8.8261	44.1306
2	35.62	0.1544	0.7720
3	40.69	0.1601	0.8004
4	50.36	10.8696	54.3478
5	55.78	9.9305	49.6524
6	61.94	0.6319	3.1596
7	64.97	0.7762	3.8808
8	66.87	0.4804	2.4018
9	70.21	0.4752	2.3762
10	83.36	1.2028	6.0140
11	89.25	0.6602	3.3012
12	116.8	1.2825	6.4127
13	121.15	1.0584	5.2921
14	128.5	3.9047	19.5236
15	130.34	0.7252	3.6261
16	132.35	4.3271	21.6357
17	156.51	6.1958	30.9789
18	178.99	27.5482	137.7410

Table 3.7: Relaxation times (T_1) determined from sub-sample s-8

No.	Chemical Shift (ppm)	T_1 (s)	5* T_1 (s)
1	21.43	9.3371	46.6853
2	35.62	0.1665	0.8326
3	40.64	0.1810	0.9049
4	50.34	9.5602	47.8011
5	55.79	9.1241	45.6204
6	61.97	0.3278	1.6391
7	64.95	0.4007	2.0034
8	66.87	0.2095	1.0473
9	-	-	-
10	83.35	1.3110	6.5548
11	89.25	0.3395	1.6976
12	116.73	0.6028	3.0139
13	121.14	0.8107	4.0535
14	128.53	2.3419	11.7096
15	130.36	0.4210	2.1052
16	133.14	1.4298	7.1490
17	157.31	3.8373	19.1865
18	178.99	27.0270	135.1351

Table 3.8: Relaxation times (T_1) determined from sub-sample s-20

No.	Chemical Shift (ppm)	T_1 (s)	5* T_1 (s)
1	21.51	8.7336	43.6681
2	36.09	0.2179	1.0894
3	40.91	0.1144	0.5721
4	50.5	8.1500	40.7498
5	-	-	-
6	63.33	0.4152	2.0761
7	65.63	0.3672	1.8359
8	-	-	-
9	-	-	-
10	-	-	-
11	-	-	-
12	-	-	-
13	-	-	-
14	129.7	-0.0077	-0.0386
15	131.49	2.9525	14.7623
16	-	-	-
17	162.5	3.0703	15.3516
18	178.99	28.4900	142.4501

Upon analysis (Tables 3.5 – 3.8) it becomes apparent that a set of T_1 values exist for the different nuclear environments in a molecule and hence depend on the progress of the reaction i.e. viscosity, molecular size and structure.

The results presented in Tables 3.5 – 3.8 indicate that a relaxation delay of greater than 25 s is required for the quantitative analysis of phenolic resins species (of interest) i.e. 5 times the longest T_1 value. However, in order to obtain an adequate integration reference signal this delay was further extended to 40 s.

3.8 DETERMINATION OF THE CONVERSION FACTORS

To relate qualitative spectra, i.e. those acquired with a short inter-pulse delay (which include the complications of additional signal enhancements (NOE)), to quantitative spectra, i.e. those acquired with a long inter-pulse delay and without additional enhancements, it was necessary to first determine both the cross calibration factor (f_c) and the NOE factor (η) for all phenolic resin species of interest within the reaction mixture.

3.8.1 Cross Calibration Factors and their Determination

The purpose of cross calibration factors is to relate the normalised integration areas calculated from NMR spectra recorded under "Rapid" and "Quantitative" conditions (see Section 2.1.2).

From the previously determined T_1 values (Tables 3.5 – 3.8), the fastest possible repetition rate could be determined based on the fastest relaxing functional group within the system. In the reaction under investigation this corresponded to the *para*, *para*-methylene bridge (40.6 ppm) having a $5T_1$ value of about 0.6 s

Under the conditions of this investigation, after a delay period of 0.6 s the sample magnetisation arising from the *para*,*para*-methylene bridge species has completely relaxed back to the equilibrium position. By applying this delay period between sequential 90º pulses, a maximum signal which gives rise to the maximum integration area possible can thus be obtained. Hence it is this delay which is employed in the "Rapid" NMR method (see Section 2.1.2).

In order to derive the cross calibration factors, two independent spectral data sets were obtained by carrying out a control reaction (see Section 2.5) and analysing the sub-samples (s-1 – s-20) under conditions of both the "Rapid" and "Quantitative" NMR methods (see Section 2.1.2).

Applying the previously determined integration ranges (see Table 3.3) to the spectral data obtained from the "Rapid" analysis of the control reaction, values for the relative rapid integration areas were thus determined (I_R). These individual integration areas were then related to the integration area of the *para,para*-methylene bridge species (I_N) (determined from within the same spectrum), resulting in their normalised integration areas (I_{RN}) (Equation 3.10):

$$I_R / I_N = I_{RN} \quad \text{..... (3.10)}$$

Similarly, application of the integration ranges to the "Quantitative" analysis of the control reaction resulted in the determination of their relative quantitative integration areas (I_Q) and normalised quantitative integration areas (I_{QN}) respectively (Equation 3.11)

$$I_Q / I_N = I_{QN} \quad \text{..... (3.11)}$$

Division of these normalised integration areas (Equations 3.10 and 3.11) results in the determination of the "cross calibration factor" (f_c) (Equation 3.12):

$$I_{RN} / I_{QN} = f_c \quad \text{..... (3.12)}$$

The cross calibration factor was then used to correct for the change in integration areas observed between the two NMR acquisition methods (i.e. Rapid and Quantitiative), resulting in a corrected integral value (I_{EN}) (Equation 3.13)

$$I_R . f_c = I_{EN} \quad \text{..... (3.13)}$$

A further correction factor was required to take into account the additional signal enhancements resulting from the "Rapid" analysis, namely the nuclear Overhauser enhancement (NOE).

3.8.2 NOE Factors and their Determination

The Nuclear Overhauser Enhancement (NOE) is the change in intensity of an NMR resonance, usually positive, when the transitions of another are saturated. The most important general consequence of the NOE is that the intensity of NMR signals can be enhanced significantly providing intensities seemingly unrelated to the concentration of species which give rise to these signals.

In ^{13}C NMR, saturation of the ^{1}H spectrum causes enhancement of protonated carbon atoms, achieved in the "Rapid" method by using power gated decoupling (see Section 2.1.4). Consequently, integration and quantification of ^{13}C NMR spectra containing NOE are generally not reliable due to these disproportionate signals. In contrast, spectra obtained using the "quantitative" method will not contain additional enhancements, as inverse gated decoupling has been employed to suppress NOE effects (see Section 2.1.3).

It is thus crucial the NOE is accounted for ensuring that a distorted result will not be obtained. The ratio of the corrected integral values obtained from the Rapid analysis (I_{EN}) to the integral values obtained from the Quantitative analysis (I_Q) led to the determination of the NOE factors (η) as employed in the present investigation (Equation 3.14).

$$\eta = I_{EN} / I_Q \quad \text{..... (3.14)}$$

3.9 APPLICATION OF THE RAPID NMR METHOD

In this section the cross calibration and NOE factors as derived above (see Section 3.8) are applied to spectral data obtained during an *in situ* phenolic resin reaction. The resulting quantitative reaction profiles enable the progress of the reaction to be monitored in real time and demonstrate the usefulness of this technique.

Upon outset of the present investigation, it was envisaged, based on previous research,[10] that spectral data acquired using the "Rapid" method i.e. non-quantitative data, could be reliably used to predict quantitative data, within an appropriate error limit (ca. 10-15%).

Equations 3.10 – 3.14 resulted in the determination of cross calibration factors (f_c) and NOE factors (η) for the 18 integration ranges (see Section 3.6), during the first 85 minutes of the reaction (i.e. sub-samples s-5 - s-9).

These factors for the integration range of *ortho*-methylol species (62 – 61.5 ppm) are presented in Table 3.9 below.

Table 3.9: A table of the cross calibration factors (f_c) and NOE factors (η) calculated for the first 85 minutes of the reaction (i.e. sub-samples s-5 – s-9) for the integration range of the *ortho* methylol phenol species (62.0 – 61.5 ppm).

Representative sub-sample	Time period (min)	f_c	η
s-5	13-38	1.137	7.34
s-6	38-53	1.219	7.313
s-7	53-63	1.166	5.78
s-8	63-75	1.227	6.133
s-9	75-85	1.197	6.319

Two methods for converting real time spectral data into quantitative data were investigated: 1) Cross calibration factors and NOE factors obtained from each of the sub-samples were averaged for the particular integration range of interest. 2) The cross calibration factors and NOE factors obtained from each of the sub-samples were used as individual factors. These allow conversion of rapid spectral data obtained from the same time period as the sub-sample

Spectral data obtained in real time using the "Rapid" method (I_{Rr}) were converted into corrected quantitative data (I_{EQr}) using Equations 3.15 and 3.16, where I_{ENr} represents the corrected intensity obtained from real time data.

$$I_{Rr} . f_c = I_{ENr} \quad \text{..... (3.15)}$$

$$I_{EQr} = I_{ENr} / \eta \quad \text{..... (3.16)}$$

These equations are analogous to Equations 3.13 and 3.14, however, in place of integration values obtained from the rapid analysis of the control reaction (as above) are the integration values obtained from the rapid analysis of the *in situ* real time reaction.

When attempting this conversion it became apparent that an additional factor, correcting for the difference in the number of scans between the two NMR methods, needed to be introduced (see Table 2.1).

The number of scans is related to signal to noise by Equation 3.4 allowing for the increase in signal to noise, due to the number of scans to be calculated. The ratio between the squares of the two values allowed for this conversion i.e. √32 / √128. Hence a correction factor (f_{NS}) of ½ was determined.

By incorporating the correction factor for the difference in the number of scans (f_{NS}) the predicted quantitative data (I_{Qr}) was calculated from the corrected quantitative data using Equation 3.17:

$$I_{Qr} = I_{EQr} . f_{NS} \quad \text{..... (3.17)}$$

The two methods of conversion (above) were used to predict quantitative data (I_{Qr}) from that obtained from the Rapid analysis of the *in situ* real time reaction (I_{Rr}). The second conversion method provided a better agreement between the predicted quantitative data (I_{Qr}) and quantitative data obtained from the individual sub-samples (I_Q) and hence this method was employed throughout this investigation.

Quantitative data were reliably predicted from spectra obtained during a real time reaction using the "Rapid" method and the above equations (Equations 3.15 – 3.17).

Although this method seems quite cumbersome at first, once the appropriate spreadsheets are set up correctly the method proves to be widely efficient (Table 3.10)

Table 3.10: The conversion from real time data (I_{Rr}) to predicted quantitative data (I_{Qr}) using the cross calibration (f_c) and NOE factors (η). Calculation shown for the fifth spectrum (of fifty) obtained during a real time reaction and for the integration range of the *ortho*-methylol phenol (62-61.50 ppm).

Spectrum	Time	I_{Rr}	f_c	I_{ENr}	η	I_{EQr}	I_{Qr}
5/50	8.4 (min)	0.297	1.137	0.3378	7.340	0.046	0.023

Figure 3.12 shows the quantitative reaction profile resulting from the conversion of the first 36 spectra (first 85 minutes of reaction) for the integration range of the *ortho*-methylol species (62.00 – 61.50 ppm).

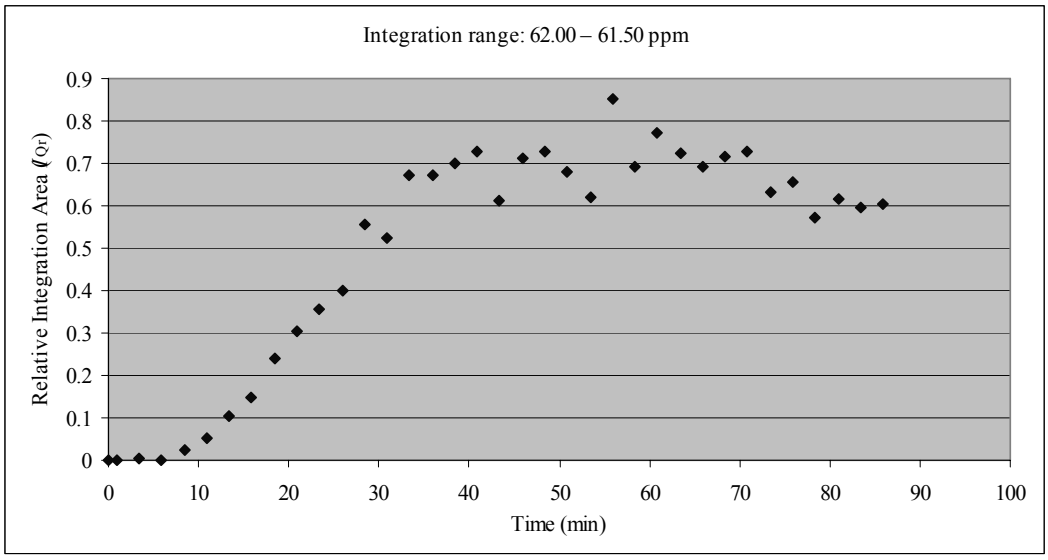

Figure 3.12: The quantitative reaction profile (after conversion) for the integration range of the *ortho* methylol species (62-61.50 ppm).

To gauge the accuracy of the predicted quantitative data and hence to assess the usefulness of this technique, the two sets of quantitative data were overlapped i.e. quantitative data obtained from the sub-samples (s-4 – s-9) (I_Q) (x) and the quantitative data predicted from the real time analysis (I_{Qr}) (♦) (Figure 3.13).

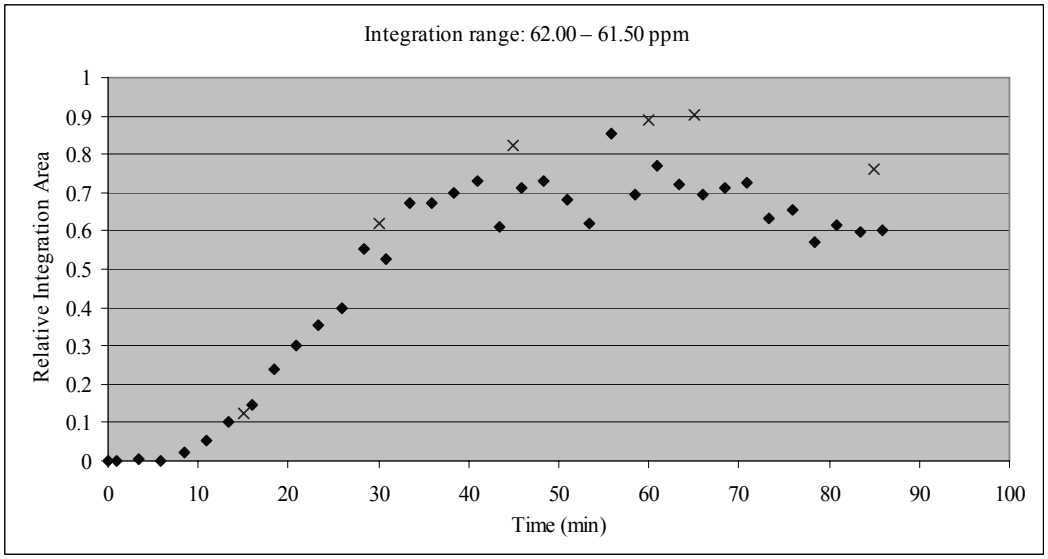

Figure 3.13: The quantitative reaction profile for the *ortho*-methylol species (♦ - real time data, x – sub-samples s-4 – s-9).

Figure 3.13 shows a reasonable correlation between the predicted quantitative data and that obtained from the control reaction. However, during the latter stages of the reaction (after about 40 min) the two lines clearly deviated from one another. This deviation was due to a combination of effects, most significantly the increase in viscosity of the reaction mixture which resulted in the NMR signals in the spectra becoming broad and disappearing below the baseline.

The effect of viscosity was also observed during the analysis of the control reaction. However, the observed signal intensities obtained from the rapid analysis of the *in situ* reaction are considerably reduced, due to the conditions of the analysis (i.e. rapid repetition rate), and hence are more prone to baseline error, thus making reliable integration difficult.

All spectral data obtained during the real time reaction were converted into quantitative data, allowing quantitative reaction profiles for each of the integration ranges to be obtained.

4 Analysis of a Phenolic Resin Reaction

4.1 INTRODUCTION

In this chapter an attempt has been made to determine the transient species present, and monitor their progress during the reaction course.

In addition to NMR, the analytical techniques of infrared spectroscopy (IR) and electrospray ionisation mass spectrometery (ES-MS) were investigated in search of additional information about the complex phenol formaldehyde reaction.

4.2 NMR REACTION MONITORING

In this section the Rapid NMR method has been applied to the analysis of an *in situ* phenolic resin reaction. Analysis of the sequential spectra obtained during this reaction provides detailed information about the sequence of reactions which occur.

In addition, the quantitative reaction profiles, as previously determined (see Section 3.9), have been employed to monitor the relative concentrations of species as a function of reaction progress and to provide information on the relative rates of formation of phenolic resin species.

Spectra obtained from the quantitative method, due to their high resolution, were used to confirm the signals obtained during the rapid analysis. This confirmation was required due to the demanding conditions of the rapid analysis and the changing nature of the reaction inevitably leading to a loss of spectral resolution.

In the present investigation the phenolic resin spectrum has been considerably simplified by omitting the complex *ipso* and aromatic regions, of which contain a significant amount of overlapping peaks and hence give rise to less reliable interpretations.

The spectral window considered was that of 100 – 25 ppm which incorporated all of the non-aromatic species present in the reaction mixture. The majority of the peaks within this range can be assigned unambiguously, while individual assignments of the signals which reside in the *ipso* aromatic regions can only be described as tentative.

Although an entire reaction was carried out *in situ*, the time period of most significance, due to the number of independent reactions occurring, was that of the first 85 minutes, hence it is this time period which is of main focus for the following section.

In the present investigation, reactions in the liquid phase are of primary importance and hence reactions involving cure can be omitted. The liquid phase reactions commonly considered are those of the addition and condensation stages, the following section deals with each of these stages of reactions separately.

4.2.1 Addition Stage Reactions

The initial reactions during a phenolic resin synthesis are generally considered to be those of methylene glycol and activated phenol, resulting in the formation of the methylol phenols (Equations 1.9 and 1.10, compounds: II and III).

However, generally only considered briefly (or omitted altogether) are those reactions of the polymeric derivatives of methylene glycol (polyoxymethylenes), resulting in the formation of essentially long-chain methylol phenols, namely the phenolic hemiformals (Figure 4.1).

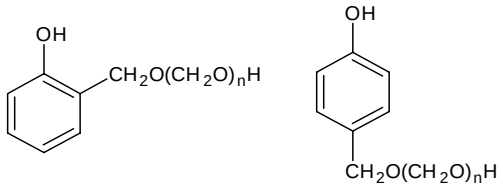

VII **VIII**

Figure 4.1: The phenolic hemiformals

Figures 4.2 and 4.3 show the consumption of unsubstituted aromatic positions and the consequent formation of the methylol and hemiformal species for the *ortho* and *para* positions respectively. The reactants were monitored as the unsubstituted positions of the phenolic ring rather than the formaldehyde type species, due to there being a number of extraneous species residing within the formaldehyde region (see Table 3.1).

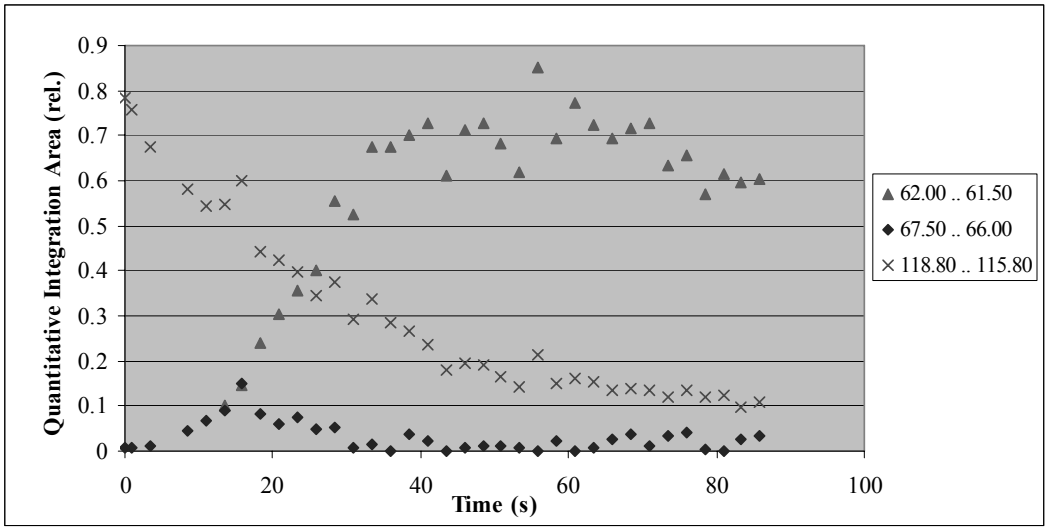

Figure 4.2: Consumption of unsubstituted *ortho* positions of the phenolic ring (118.8-115.8 ppm) and the subsequent formation of the *ortho*-methylol (62-61.5 ppm) and *ortho*-hemiformal species (67.5-66 ppm).

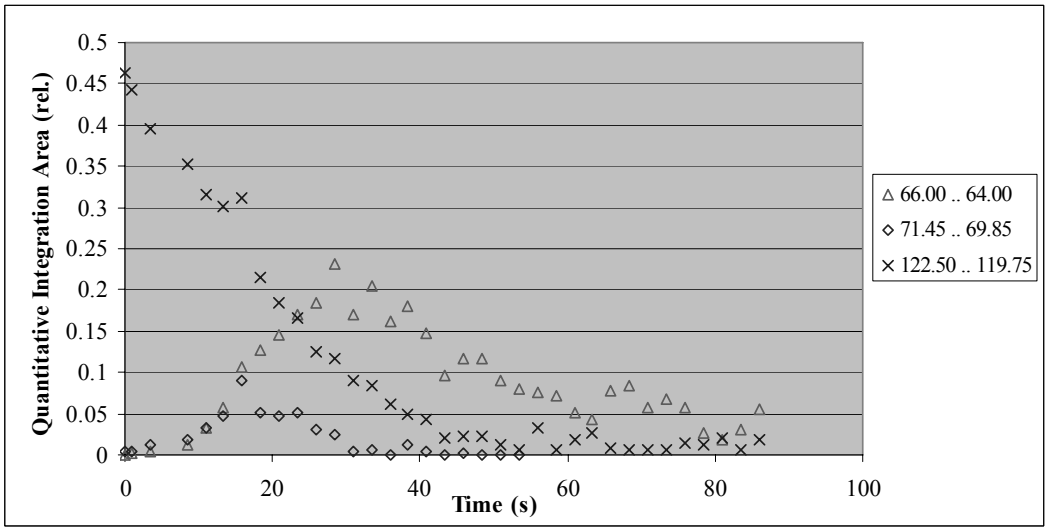

Figure 4.3: Consumption of unsubstituted *para* positions of the phenolic ring (122.5-119.75 ppm) and the subsequent formation of the *para*–methylol (66-64 ppm) and hemiformal species (71.45-69.85 ppm).

The methylol phenols undergo further reactions to form the di-methylol phenol derivatives (Equation 1.12 and 1.13, compounds IV and V); similar reactions are assumed resulting in the formation of the di-hemiformal species (Figure 4.4).

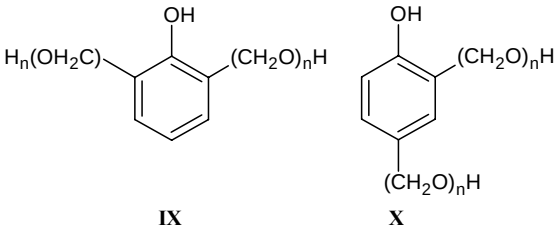

IX **X**

Figure 4.4: The di-hemiformal species

No evidence of the 2,6-dihemiformal species (IX) was found under the conditions of the present investigation. However, this compound is likely to form and analogous to the 2,6-dimethylol phenol (V), is presumed to be highly reactive and *para* directing.[37]

The signals arising from the mono- and di-hemiformal species appear overlapped in the rapid NMR spectrum. The high resolution of the quantitative method allows for the identification of the two independent signals (Figure 4.5).

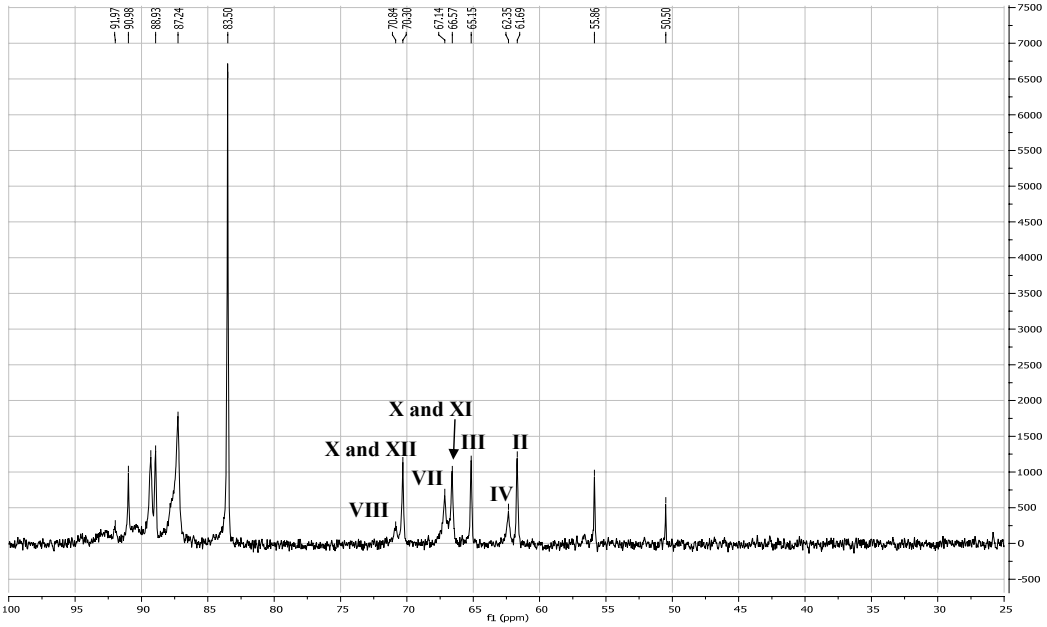

Figure 4.5: A quantitative NMR spectrum showing the reaction products of the addition stage reactions (sub-sample s-4).

The possibility now arises whereby the dimeric product can have substituents of different chain lengths. Mixtures of these dimeric products create complication upon analysis due to the similarity of these subsituents i.e. when monitoring the *para*-hemiformal, compound X cannot be readily distinguished from compound XII. Similar problems exist for the *ortho* compound (see Figure 4.6).

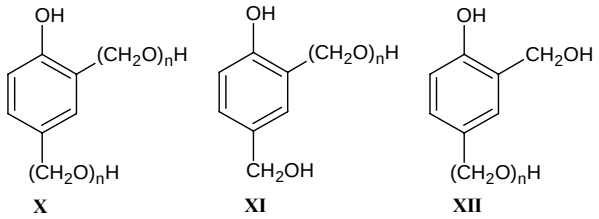

Figure 4.6: The possible variants of the dimeric species observed.

It is known that di-methylol phenols react to form the tri-methylol derivative (Equation 1.13 (VI)). However, further reactions of the di-hemiformal species resulting in the formation of the tri- hemiformal derivative are unlikely due to effects of steric crowding.

The relative rates of formation of these first reactions were observed by normalising the maximum intensities of the individual reaction profiles to a common value, in this case one (Figure 4.7). The slope of the individual reaction profile now becomes proportional to the rate of formation for that individual functional group.

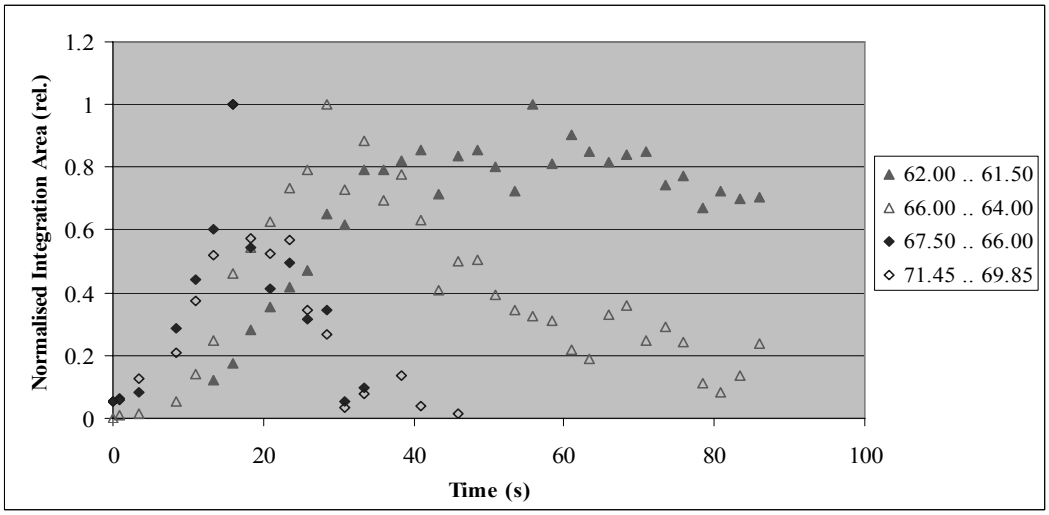

Figure 4.7: Normalised reaction profiles of the addition stage reaction products i.e. the *ortho*- and *para*-methylol phenols (62-61.5 ppm and 66-64 ppm respectively), and the *ortho*- and *para*-hemiformals (67.5-66 ppm and 71.45-69.85 ppm respectively).

It was clearly observed (Figure 4.7) that the initial reaction products are those of the transient phenolic hemiformals. The next major species to form were those of the methylol phenols, initially the *para* methylol phenol followed by the *ortho* methylol. It appears that the *para* aromatic carbon was more reactive towards formaldehyde (and its oligomeric forms) than the *ortho* aromatic carbon. This observation is in close agreement with the literature.[37]

However the *para* methylol phenol can now be seen reacting out of the medium, leading to the predominance of the *ortho* methylol signal. The stabilisation of the *ortho* methylol phenol has previously been described as a consequence of intramolecular hydrogen bonding between the methylol and adjacent hydroxyl group of phenol.[35]

4.2.2 Condensation Stage Reactions

As a result of condensation reactions, resonances associated with the formation of *para,para*- and *ortho,para*-methylene bridges begin to appear (Figure 4.8). However no spectral evidence of the *ortho,ortho*-methylene bridges was observed (~30 ppm) as these species are unlikely to form under the alkaline conditions of of the present investigation.

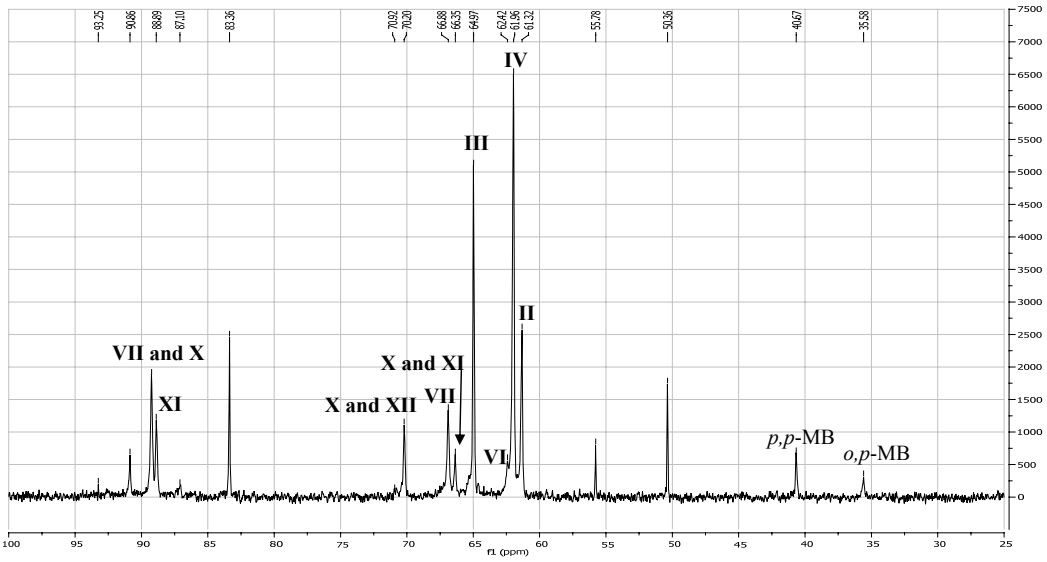

Figure 4.8: A quantitative NMR spectrum showing the reaction products of the condensation stage reactions (sub-sample .s-5)(*para,para*- and *otho,para*-methylene bridges have been denoted as *p,p'*-MB and *o,p'*-MB respectively).

The condensation reactions leading to the formation of methylene bridges are generally considered to be those involving the methylol phenols (Equations 1.5 – 1.7). However Figure 4.9 shows that after the first 20 minutes of the reaction the formation of the methylol species and methylene bridges occur simultaneously, with only the *para* methylol species showing any tendency to react out of the system.

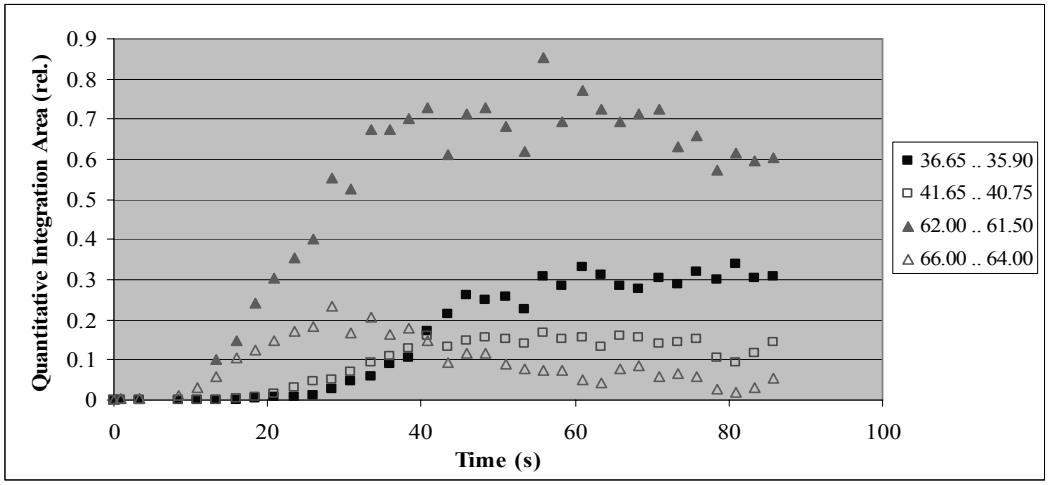

Figure 4.9: The reaction profiles for the *ortho* and *para*-methylol species (62-61.5 and 66-64 ppm respectively) and the *ortho,para*- and *para,para*-methylene bridge species (36.65-35.9 and 41.65-40.75 ppm respectively).

Figure 4.10 shows the reaction profiles of the hemiformal and methylene bridge species. Upon analysis it appears likely that the hemiformal species play a significant role in these condensation reactions.

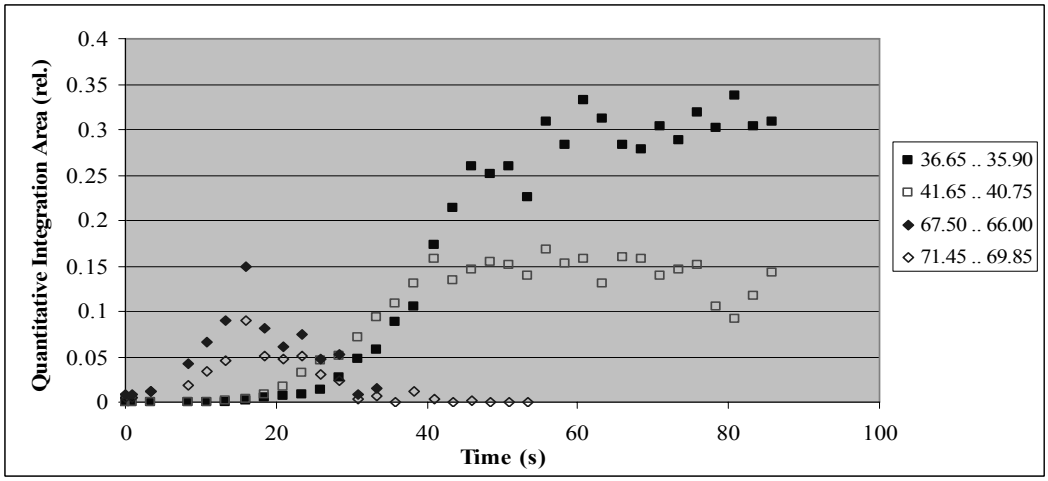

Figure 4.10: The reaction profiles for the *ortho*- and *para*-hemiformal (67.5-66 and 71.45-69.85 ppm) and the *otho,para*- and *para,para*- methylene bridge species(36.65-35.9 and 41.65-40.75 ppm respectively).

In order to explain this phenomena, parallel reactions leading to the formation of methylol groups and methylene bridges must be present. The reactions involved in the consumption of the phenolic hemiformals are here considered to be analogous to those of the methylol phenols (Equations 1.5 and 1.7). Thus the proposed mechanisms for the self condensation of the phenolic hemiformals resulting in the formation of the *ortho,para*- and *para,para*-methylene bridges are shown in Equations 4.1 and 4.2 respectively.

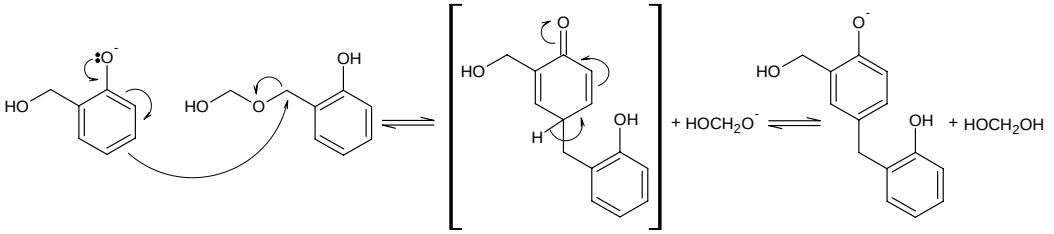

..... (4.1)

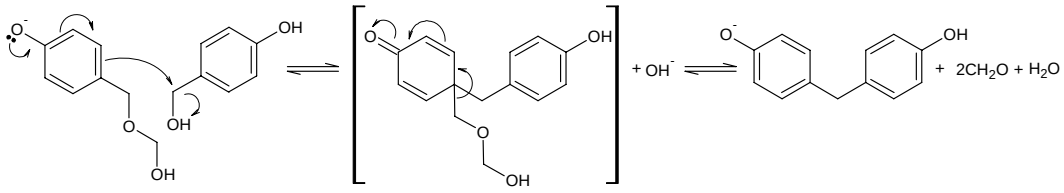

..... (4.2)

Figure 4.11 shows that the initial condensation reactions favour the *para* position leading to their dominance during the early stages of the reaction. Further condensation reactions, due to the limited number of reactive *para* sites available, lead to the formation of the *ortho,para*-methylene groups and eventually lead to their dominance.

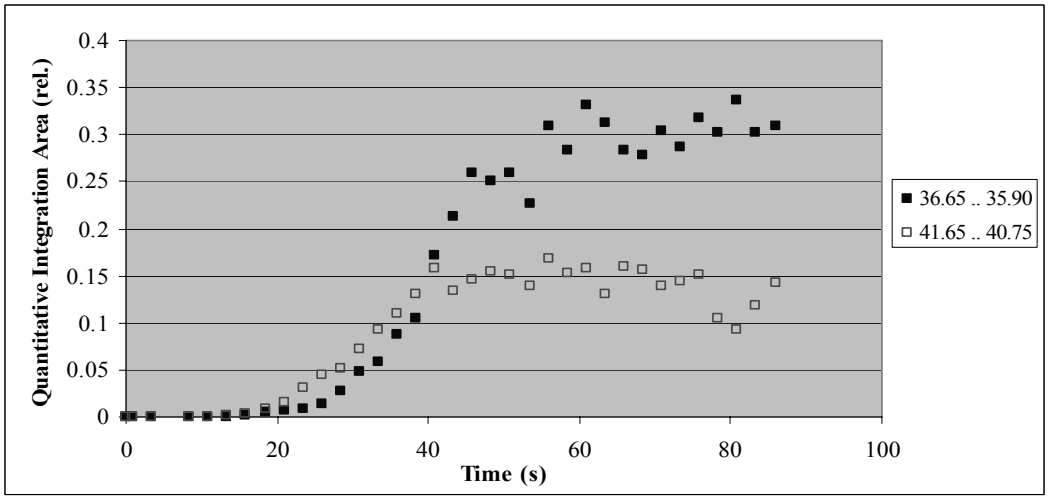

Figure 4.11: The reaction profiles for the *ortho,para*- and *para,para*-methylene bridge species (36.65-35.9 and 41.65 and 40.75 ppm respectively).

4.2.3 Parallel Reactions

Due to the consumption of formaldehyde (and its associated oligomers) the equilibrium between the hemiacetals and methylene glycol (Equation 1.6) is considerably offset. In an attempt to balance this equilibrium the hemiacetal type species react out of the system to form methanol and methylene glycol. This reaction was observed directly as an increase in methanol; however the increase in methylene glycol was masked by the various formaldehyde consuming reactions occurring simultaneously.

The condensation reactions (Section 4.2.2) lead to the formation of formaldehyde and hence a build up of formaldehyde (as methylene glycol) has been observed late in the reaction. During these late stages of the reaction the majority of the reactive positions on the phenolic ring have been saturated and hence this "free formaldehyde" resides in the reaction mixture.

The condensation reactions proposed above take place at the α position of the hemiformal (Equation 4.1). Thus it seems reasonable to assume the reaction can also take place at the β position (Equation 4.3). The following is a proposed self condensation mechanism resulting in the formation of dimethylene ether bridges (DMEB).

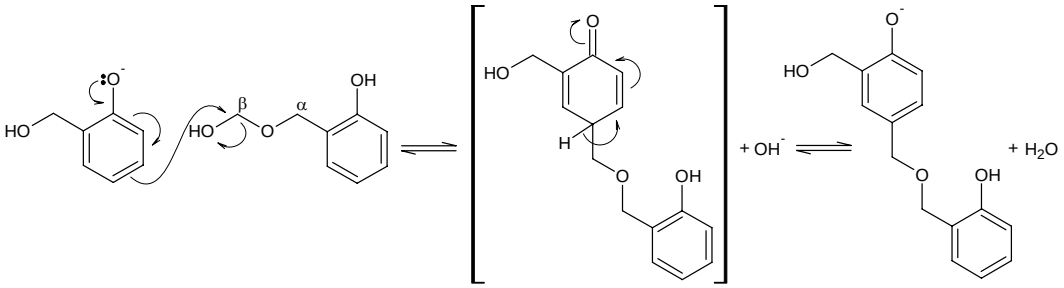

..... (4.3)

However under the conditions of this investigation (strongly alkaline) this reaction is unlikely to proceed, however these species are generally related to curing type reactions and may become important during later stages of the reaction.

4.3 OTHER TECHNIQUES

Although the present investigation was mainly dedicated to the ^{13}C NMR analysis of phenol formaldehyde resin, some additional techniques were investigated to observe if any complementary information could be obtained. These techniques were: infrared spectroscopy (IR) and electrospray ionisation mass spectrometry (ES-MS).

4.3.1 Fourier Transform Infrared Spectroscopy

Fourier transform infrared spectroscopy (FT-IR) was investigated as a complementary technique to NMR due to its sensitivity. ATR and conventional thin film infrared spectroscopy techniques were employed for the characterisation of the sub-samples s-1 – s-6 (see Section 2.5.2).

It was initially thought that ATR could provide additional benefits to the analysis; however spectra obtained from the two techniques were very similar. The phenolic resin samples as prepared in this investigation were thus run as thin films between CaF_2 windows, due to the ease of this technique.

A representative IR spectrum is given in Figure 4.12 below:

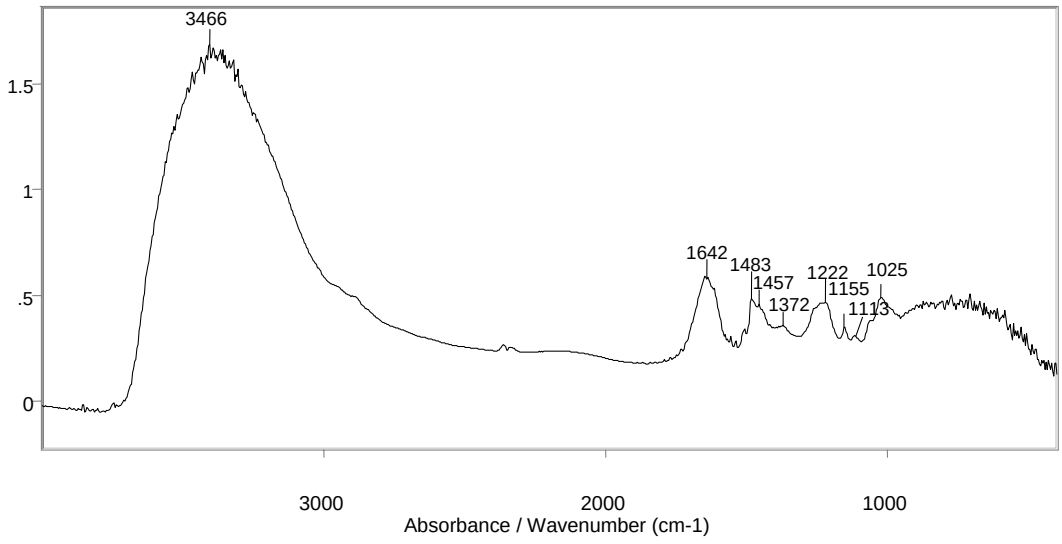

Figure 4.12: A representative FT-IR spectrum of a phenolic resin sample (sub-sample s-4).

All major FT-IR signals were assigned in accordance with the presented literature values,[21, 22] a table of such assignments is presented below (Table 4.1).

Table 4.1: Assignments of phenolic resin absorptions (ν-stretch, *d*- deformation or bend, *ip*- in-plane, *op*- out of plane).

Nature	Assignment	Wavenumber (cm^{-1})
Phenolic and methylol (broad)	ν(OH)	3460
Aromatic	ν(CH)	3060
Aromatic	ν(CH)	3020
Aliphatic	$\nu_{ip}(CH_2)$	2930
Aliphatic	$\nu_{op}(CH_2)$	2860
Benzene ring	ν(C=C)	1640
Benzene ring	ν(C=C)	1480
Aliphatic	$d(CH_2)$	1470
Benzene ring	ν(C=C)	1450
Phenolic	d_{ip}(OH)	1370
Phenolic	ν(C-O)	1240
Aromatic	d_{ip}(CH)	1150
Methylol	*d*(C-O-C)	1110
Methylol	ν(C-O)	1030

The infrared spectra of the resin samples, as prepared in the present investigation were dominated by the large OH stretch which encompasses signals related to the hydroxyl group of the phenolic ring, those of water and also the terminal hydroxyl groups of the methylene glycol and methylol type groups. A ridge appears to the right of this and has been assigned to the various stretching modes of both the aromatic methine and aliphatic methylene signals.

In order to provide details of the complex phenolic resin reaction, not easily obtained from this region, the "finger print" region (2000 – 400 cm^{-1}) of the phenolic resin infrared spectrum was investigated (Figure 4.13).

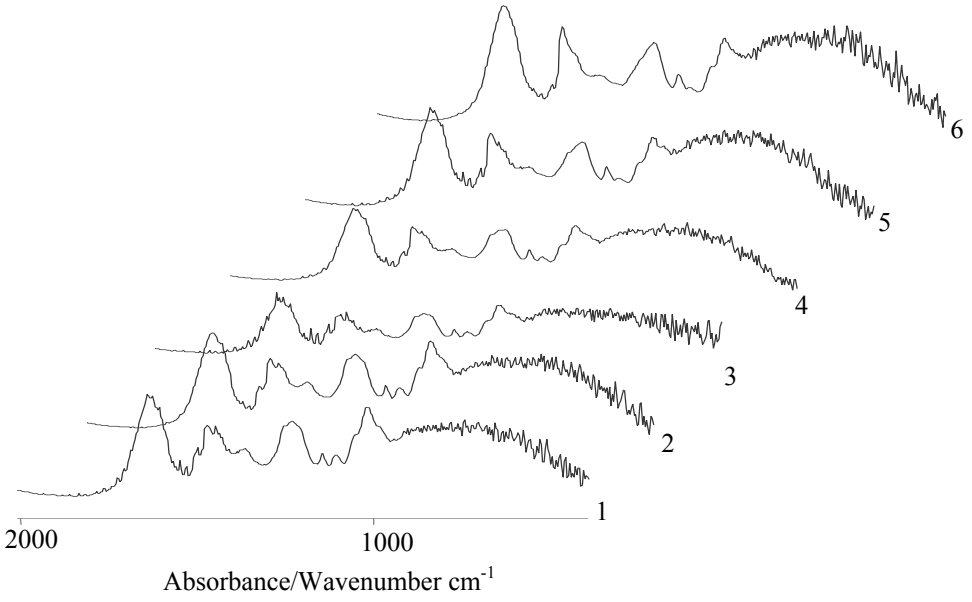

Figure 4.13: IR analysis of the "finger print" region (2000 – 400 cm^{-1}) for the samples s-1 – s-6.

The series of infrared spectra obtained (Figure 4.13) show several of the key reactions taking place. A decrease in the C-O-C deformation at approximately 1110 cm^{-1} corresponds to the decrease in formaldehyde type species upon forming methylene bridges and hence an associated increase in the aliphatic CH_2 deformation at approximately 1470 cm^{-1} can be observed. The broad peak at approximately 1030 cm^{-1} tends to shift to a higher wavenumber value as the reaction proceeds. This phenomenon has previously been assigned to the effects of intermolecular hydrogen bonding due to the presence of one or more methylol type species at the ortho position of the phenolic ring.[22]

Although analysis of the "finger print" region was found to provide information about the reactions occurring during a phenolic resin reaction, the spectra appears complex and overlapping signals are common, leading to less reliable interpretation.

4.3.2 Electrospray Ionisation Mass Spectrometry

Electrospray ionisation mass spectrometry (ES-MS) was used to investigate the reaction of phenolic resins in order to resolve the oligomer distribution. ES-MS spectra were obtained for sub-samples s-1 and s-3 taken during the control reaction.

Under the conditions of analysis neutral complexes M can ionise with a solution cation (X^+) to give $[M + X]^+$ positive ions. In the case of phenolic resins the cation is typically a proton (H^+) or a sodium ion (Na^+). Figure 4.14 shows the well resolved series of mass spectral peaks ($[M + X]^+$ ions) obtained from the ES-MS analysis of sample s-1 (essentially the initial reaction mixture).

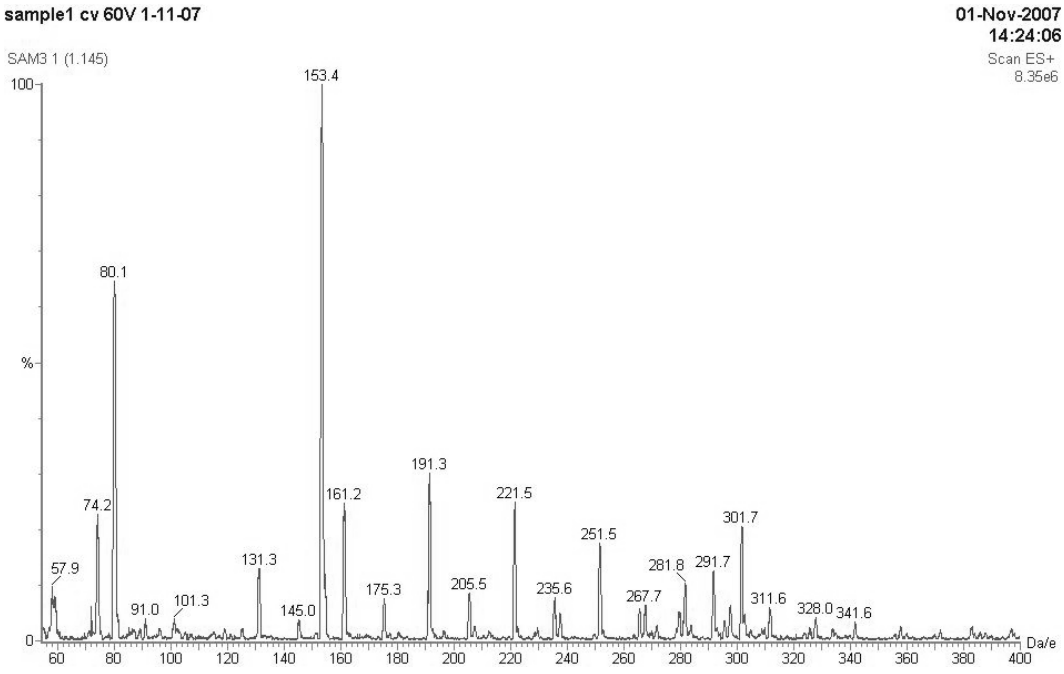

Figure 4.14: ES-MS spectrum of sub-sample s-1, the initial reaction mixture.

The dominant peaks at *m/z* 80.1 and 153.4 were assigned to solvated methylene glycol ($[M + CH_3OH]^+$) and phenol ($[M + (H_2O)_2 + Na]^+$) respectively.
The polymeric methylene glycol ($HO(CH_2O)_nH$) and phenolic hemiformal ($H_3CO(CH_2O)_nH$) species show characteristic $[M + Na]^+$ molecular ions and distinctive peak to peak mass increments of 30 Daltons (Da). These increments correspond to longer chain oligomers (where, n = 2 – 9) with the addition of one formaldehyde unit (CH_2O).

Figure 4.15 shows the complex mass spectrum obtained from the analysis of sample s-3.

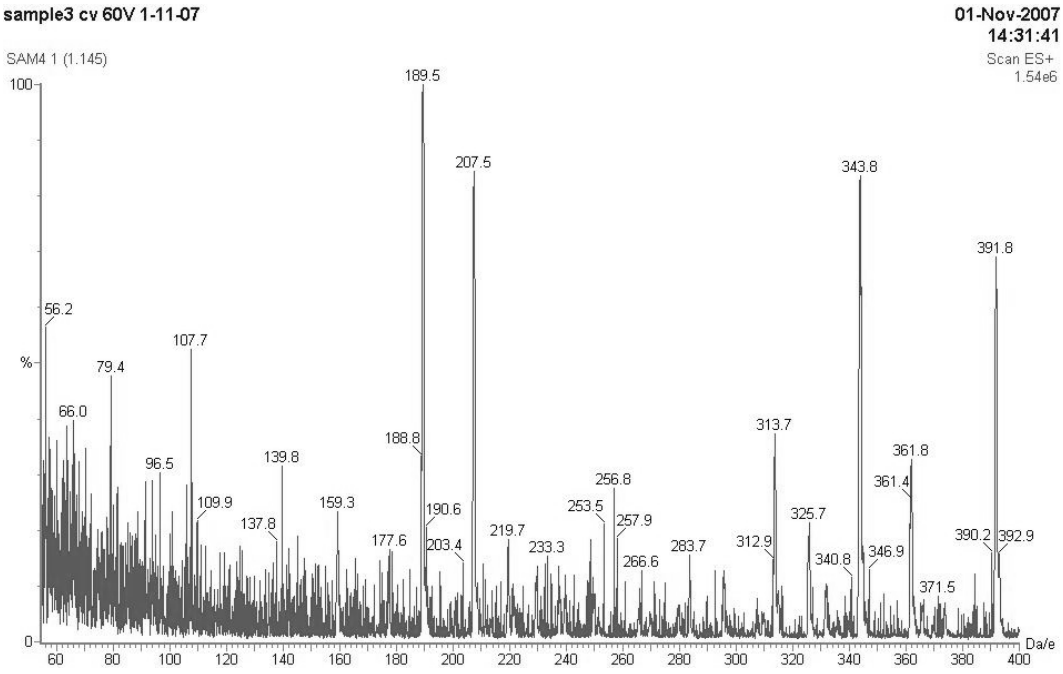

Figure 4.15: ES-MS spectrum of sample s-3

The weak *m/z* 177 ion observed in this spectrum is believed to correspond to a phenolic moiety bound to two formaldehyde units $[M + Na]^+$, while the *m/z* 207 ion is believed to arise from a phenolic residue with three attached formaldehyde units.

Several isomer forms of products with $[M + Na]^+$ ions at *m/z* 177, 207, etc. are possible. A limitation of ES-MS is that individual oligomers cannot be unequivocally identified in the ES-MS spectrum i.e. it is not possible to assign a single chemical structure to the 177 *m/z* $[M + Na]^+$ molecular ion (Figure 4.16)

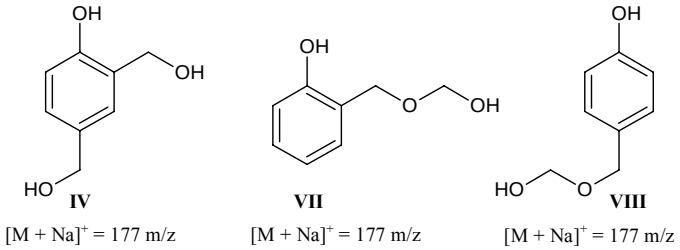

Figure 4.16: The isobar masses possible for the 177 *m/z* ion.

A second series of peaks ($[M + Na]^+$ ions) was observed for species which differed by from the foregoing series of peaks by106 Daltons. This mass increase corresponds to the addition of phenolic ring via a methylene bridge leading to species which showed $[M + Na]^+$ ions at *m/z* 283, 313 and 343 (corresponding to the presence of 1, 2 and 3 formaldehyde units respectively).

A further series ions at *m/z* 159.3, 189.5, and 219.7 show peak to peak mass increments of 30 Da and 106 Da (as above), however these ions could not be assigned in the present investigation.

ES-MS provides detailed information about the oligomeric distribution of phenolic resin species. However in the presence of compounds with isobar masses assignments of individual oligomers becomes tentative.

5 General Discussion and Conclusions

5.1 GENERAL DISCUSSION

The novel NMR acquisition methods previously applied to urea formaldehyde resins by Zeng,[10] were here taken and developed further for the analysis of the complex phenol formaldehyde resin system.

In the past, commercial formulations for phenolic resins have been developed almost entirely on an empirical basis. Further development has therefore necessitated a more complete understanding of how these resins are formed and function. This NMR acquisition method provides direct insight into the polymerisation reactions taking place during synthesis. This is achieved by providing intimately spaced spectra (ca. 2.5 min intervals) which correspond to snapshots of the reactions progress in real time.

Conventional NMR techniques have been used widely for the analysis of phenolic resin system. However these techniques are time consuming and in practice can obtain information about the final resin, and only a limited number of stages during the reaction.

A more direct approach to the analysis was achieved by *in situ* monitoring, whereby the reactants were added directly into an NMR tube and the reaction commenced inside the NMR spectrometer. Adequate mixing of the reactants during synthesis may be a problem in the spinning NMR tube within spectrometer. For the purposes of the present work it was assumed that convective stirring was sufficient to allow heat flow out of the tube so that localised overheating did not occur.

In the past these *in situ* experiments have been carried out under isothermal conditions. However in the present investigation the *in situ* phenolic resin reaction was carried out over a range of temperatures, closely imitating those employed during a typical commercial synthesis, a consideration not often achieved in the literature.

While this regime makes theoretical interpretation more difficult, it more realistically represents what happens in a commercial synthesis and provides a more relevant tool for empirical optimisation of conditions.

Therefore knowledge of the sample temperature during the reaction and precise control of the temperature increments was necessary. Differences in temperature programmed and actually observed by the sample will cause the polymerisation reaction to proceed at different rates; higher temperatures will cause the reaction to proceed more quickly than anticipated and cause the resin mixture to gel.

In situ reaction monitoring provides the advantage of real time NMR analysis, allowing the sequence of structures to be determined as a function of time and qualitative reaction profiles to be obtained. However due to the nature of the reaction conventional NMR techniques are employed with non-ideal relaxation delays (short) and broadband decoupling. The consequence of broadband decoupling is that signals appear with an additional NOE enhancement. This enhancement proves beneficial when attempting to identify signals which may otherwise be lost beneath the baseline however, detrimental when attempting quantification.

If an NMR experiment is carried out under quantitative conditions the individual signals within the NMR spectrum are directly proportional to the concentration of carbon atoms giving rise to those signals. The most important general consequence of the NOE is that the intensity of NMR signals can be enhanced significantly providing intensities seemingly unrelated to the concentration of species which give rise to these signals.

The advancement of the present investigation allowed spectral data obtained from these seemingly unrelated intensities (qualitative) to be converted into quantitative spectral data. This quantification allows the concentration of individual species to be monitored as a function of time and hence allows quantitative reaction profiles to be obtained.

In contrast to Zeng's work which relied strongly on the theoretical manipulation and estimation of signal intensities, this project by comparison was more empirically based and hence focussed mainly on the processing of experimental data.

Two NMR data acquisition methods were developed, depicted as "The Quantitative Method" and "The Rapid Method". The two methods differ significantly in the way in which spectra are obtained; the most notable differences being the acquisition time and pulse repetition rates.

Generally for quantitative NMR measurements the repetition rate should be in the order of five times the relaxation time (T_1) of the *slowest* relaxing functional group within the system, when using a 90º pulse. The rate at which individual Rapid NMR experiments can be repeated is however limited by the relaxation time (T_1) of the *fastest* relaxing functional group within the system. The overall acquisition time is then governed by the number of repetitions required to achieve adequate signal to noise.

In order to obtain the optimum repetition rates for the two individual NMR acquisition methods, the relaxation times of various phenolic resin species were determined using the inversion recovery method.

A sub-sampling method was employed to provide samples at various stages of a commercial type control reaction. By relating spectral data obtained from these samples analysed using the Rapid and Quantitative methods, the cross calibration and NOE factors were derived.

Real time NMR spectral data obtained during an *in situ* reaction (via the Rapid NMR acquisition method) were normalised to that of the fastest relaxing functional group within the system. The application of these cross calibration and NOE factors thus allowed this spectral data to be quantified, an essential component for meaningful kinetic studies.

A reasonable correlation between the predicted quantitative data and that obtained from the control reaction was observed. However during the later stages of the reaction due to an increase in viscosity, the resulting NMR signals become broad and disappear below the baseline, thus making reliable integration difficult. Hence deviations between the two quantitative data sets become apparent.

5.2 CONCLUSIONS

In conclusion, the novel NMR acquisition methods previously presented by Zeng can be taken and developed further for new resin systems. In the present investigation these methods have been developed for the phenolic resin system.

The main parameters which need to be taken into consideration when applying these methods to a new resin system are the longitudinal relaxation time (T_1) and the nuclear Overhausser enhancement (NOE). Without prior knowledge of these parameters the fastest possible repetition rates for Rapid and Quantitative methods cannot be established and hence correlations between qualitative and quantitative spectral data cannot be drawn.

The present investigation shows the development an NMR method capable of identifying and quantifying the sequential structures present and monitoring their concentration changes during an *in situ* phenoic resin preparation.

This investigation has provided the foundation for further research in the field of quantitative *in situ* reaction monitoring of phenolic resin and will help to provide new information about how to optimise phenolic resin adhesives that are supplied to the Plywood and LVL industries.

5.3 FURTHER DEVELOPMENT

Further development and extension of this work will allow the effects of varying synthesis parameters (i.e. temperature, stoichiometry, pH, catalyst etc.) on the structure and hence on the physical properties to be determined. These determinations will allow relationships between the chemical structure and the physical properties of the resin to be made, inevitably leading to the optimisation of the reaction conditions. This would be seen as invaluable so that new; more innovative and cost-effective resins can be developed.

The methods applied in the present investigation along with the knowledge of relaxation times and NOE factors, could be further extended and adapted to the analysis of new resin systems.

References

1. Knop, A.; Scheib, W., *Chemistry and Application of Phenolic Resins*. Springer-Verlag Berlin Heidelberg New York: 1979.

2. Baekeland, L. H. Method of Making Insoluble Products of Phenol and Formaldehyde. 1909.

3. EDGAR online, Hexion Specialty Chemicals, Inc. Quarterly Report (10-Q). In 2007.

4. Megson, N. J. L., *Phenolic Resin Chemistry*. Butterworths Scientific Publications: 1958.

5. Gardziella, A.; Pilato, L. A.; Knop, A., *Phenolic Resins, Chemistry, Applications, Standardization, Saftey and Ecology*. 2nd ed.; Springer-Verlag: Berlin, 2000.

6. Saunders, K. J., *Orgainc Polymer Chemistry*. 2nd ed.; Chapman and Hall: 1988.

7. Chenier, P. J., *Survey of Industrial Chemistry*. Second ed.; VCH: 1992.

8. Stevens, M. P., *Polymer Chemistry: An Introduction*. Third ed.; Oxford University Press: 1999.

9. Nicholson, J. W., *The Chemistry of Polymers*. Third ed.; RSC Publishing: 2006.

10. Zeng, H. Studies of the Formation and Properties of Urea-Formaldehyde Resin Adhesives. The University of Waikato, Hamilton, New Zealand, 2001.

11. Freeman, J. H.; Lewis, C. W., Alkaline-catalyzed Reaction of Formaldehyde and the Methylols of Phenol; A Kinetic Study. *Journal of the American Chemical Society* **1953,** 72, 2080-2087.

12. Fyfe, C. A.; Rudin, A.; Tchir, W., Application of High-Resolution ^{13}C NMR Spectroscopy Using Magic Angle Spinning Techniques to the Direct Investigation of Solid Cured Phenolic Resins. *Macromolecules* **1980,** 13, 1320 - 1322.

13. Chuang, I. S.; Maciel, G. E., ^{13}C NMR Investigation of the Stability of a Resol-Type Phenol-Formaldehyde Resin toward Formalin, toward Base, and toward Nonoxidizing or Oxidizing Acid. *Macromolecules* **1991,** 24, 1025 - 1032.

14. Derome, A. E., *Modern NMR Techniques for Chemistry Research*. Pergamon Press: 1987.

15. Breitmaier, E.; Voelter, W., *Carbon-13 NMR Spectroscopy*. Third ed.; VCH: 1987.

16. Field, L. D.; Sternhell, S., *Analytical NMR*. John Wiley & Sons: 1989.

17. Freeman, R., *Magnetic Resonance in Chemistry and Medicine*. Oxford University Press: 2003.

18. Li, P.; Coleman, D. W.; Spaulding, K. M.; McClennen, W. H.; Stafford, P. R.; Fife, D. J., Fractionation and Characterization of Phenolic Resins by High-Performance Liquid Chromatography and Gel-Permeation Chromatography Combined with Ultraviolet, Refractive Index, Mass Spectrometry and Light-Scattering Detection. *Journal of Chromatography A* **2001,** 914, 147 - 159.

19. Astarloa-Aierbe, G.; Echeverria, J. M.; Egiburu, J. L.; Ormaetxea, M.; Mondragon, I., Kinetics of phenolic resol resin formation by HPLC. *Polymer* **1998,** 39, (14), 3147.

20. Holopainen, T.; Alvila, L.; Rainio, J.; Pakkanen, T. T., Phenol - Formaldehyde Resol Resins Studied by ^{13}C-NMR Spectroscopy, Gel Permeation Chromatography, and Differential Scanning Calorimetry. *Journal of Applied Polymer Science* **1997,** 66, 1183 - 1193.

21. Holopainen, T.; Alvila, L.; Rainio, J.; Pakkanen, T. T., IR Spectroscopy as a Quantitative and Predictive Analysis Method of Phenol-Formaldehyde Resol Resins. *Journal of Applied Polymer Science* **1998,** 69, 2175-2185.

22. Poljansek, I.; Sebenik, U.; Krajnc, M., Characterization of Phenol-Urea-Formaldehyde Resin by Inline FTIR Spectroscopy. *Journal of Applied Polymer Science* **2006,** 99, 2016-2028.

23. Pizzi, A.; Pasch, H.; Simon, C.; Rode, K., Structure of Resorcinol, Phenol, and Furan Resins by MALDI-TOF Mass Spectrometry and ^{13}C NMR. *Journal of Applied Polymer Science* **2004,** 92, 2665 - 2674.

24. Schrod, M.; Rode, K.; Braun, D.; Pasch, H., Matrix-Assisted Laser Desorption/Ionization Mass Spectrometry of Synthetic Polymers. VI. Analysis of Phenol-Urea-Formaldehyde Cocondensates. *Journal of Applied Polymer Science* **2003,** 90, 2540 - 2548.

25. de Breet, A. J. J.; Dankelman, W.; Huysmans, W. G. B.; de Wit, J., ^{13}C-NMR Analysis of Formaldehyde Resins. *Die Angewante Makromolekulare Chemie* **1977,** 62, 7 - 31.

26. Kim, M. G.; Tiedeman, G. T.; Amos, L. W., Carbon-13 NMR Study of Phenol-Formaldehyde Resins. *Weyerhaeuser Science Symposium, Phenolic Resins, Chemistry and Application* **1979,** 2, 262 - 289.

27. Bouajila, J.; Raffin, G.; Waton, H.; Sanglar, C.; Paisse, J. O.; Grenier-Loustalot, M., Phenolic Resins - Characterizations and Kinetic Studies of Different Resols Prepared with Different Catalysts and Formaldehyde/Phenol Ratios (I). *Polymers and Polymer Composites* **2002,** 10, (5), 341 - 359.

28. Rego, R.; Adriaensens, P. J.; Carleer, R. A.; Gelan, J. M., Fully Quantitative carbon-13 NMR characterization of resol phenol-formaldehyde prepolymer resins. *Polymer* **2004,** 45, 33-38.

29. Grenier-Loustalot, M. F.; Larroque, S.; Grande, D.; Grenier, P.; Bedel, D., Phenolic Resins: 2. Influence of Catalyst Type on Reaction Mechanisms and Kinetics. *Polymer* **1996,** 37, (8), 1363 - 1369.

30. Luukko, P.; Alvila, L.; Holopainen, T.; Rainio, J.; Pakkanen, T. T., Effect of Alkalinity on the Structure of Phenol-Formaldehyde Resol Resins. *Journal of Applied Polymer Science* **2001,** 82, 258 - 262.

31. Werstler, D. D., Quantitative ^{13}C N.M.R. Characterization of Aqueous Formaldehyde Resins: 1. Phenol-Formaldehyde Resins. *Polymer* **1986,** 27, 750 - 756.

32. Kim, M. G.; Amos, L. W.; Barnes, E. E., Study of the Reaction Rates and Structures of a Phenol-Formaldehyde Resol Resin by Carbon-13 NMR and Gel Permeation Chromatography. *Industrial and Engineering Chemistry Research* **1990,** 29, (10), 2032-2037.

33. Monni, J.; Alvila, L.; Pakkanen, T. T., Structural and Physical Changes in Phenol-Formaldehyde Resol Resin, as a Function of the Degree of Condensation of the Resol Solution. *Industrial and Engineering Chemistry Research* **2007,** 46, 6916 - 6924.

34. Sojka, S. A.; Wolfe, R. A.; Guenther, G. D., Formation of Phenolic Resins: Mechanism and Time Dependence of the Reaction of Phenol and Hexamethylenetetramine As Studied by Carbon-13 Nuclear Magnetic Resonance and Fourier Transform Infrared Spectroscopy. *Macromolecules* **1981,** 14, 1539 - 1543.

35. Pethrick, R. A.; Thomson, B., ^{13}C Nuclear Magnetic Resonance Studies of Phenol-Formaldehyde Resins and Related Model Compounds. 2-Analysis of Sequence Structure in Resins. *British Polymer Journal* **1986,** 18, (6), 380 - 386.

36. Haupt, E., A Timesaving Method to Determine the Length of a 90º Pulse. *Journal of Magnetic Resonance* **1982,** 49, (2), 358 - 364.

37. Grenier-Loustalot, M.; Larroque, S.; Grenier, P.; Leca, J.; Bedel, D., Phenolic Resins: 1. Mechanisms and Kinetics of Phenol and of the First Polycondensates Towards Formaldehyde in Solution. *Polymer* **1994,** 35, (14), 3046 - 3054.

38. Fisher, T. H.; Chao, P.; Upton, C. G.; Day, A. J., One- and Two-Dimensional NMR Study of Resol Phenol-Formaldehyde Prepolymer Resins. *Magnetic Resonance in Chemistry* **1995,** 33, 717-723.

39. Fisher, T. H.; Chao, P.; Upton, C. G.; Day, A. J., A ^{13}C NMR study of the methylol derivatives of 2,4'- and 4,4'-dihydroxydiphenylmethanes found in resol phenol-formaldehyde resins. *Magnetic Resonance in Chemistry* **2002,** 40, 747-751.